THE EFFECTS OF SKIN-TISSUE MORPHOMETRY ON THE MECHANICAL IMPEDANCE OF RAT GLABROUS SKIN

by

Çağlar Gök

B.S., Biology, Çukurova University 2009

B.S., Chemistry, Çukurova University 2009

Submitted to the Institute of Biomedical Engineering

in partial fulfillment of the requirements

for the degree of

Master of Science

in

Biomedical Science

Boğaziçi University

2012

THE EFFECTS OF SKIN-TISSUE MORPHOMETRY ON THE MECHANICAL IMPEDANCE OF RAT GLABROUS SKIN

APPROVED BY:

Assoc. Prof. Dr. Burak Güçlü .....
(Thesis Advisor)

Assoc. Prof. Dr. Can Yücesoy .....

Assist. Prof. Dr. Necla Birgül-İyison .....

DATE OF APPROVAL: 10 September 2012

ACKNOWLEDGMENTS

I'm grateful to my family for their support and encouragement during my master study.

I specially thank to my advisor Burak Güçlü for his support, help and motivation during all stages of the thesis.

I thank to Assoc. Prof. Dr. Can Yücesoy and Assist. Prof. Dr. Necla Birgül-İyison for their precious comments. I also thank to İsmail Devecioğlu, Ahu Türkoğlu, Yetiş Gültekin, Shervin Bashiri and Sedef Yusufoğulları for their help.

ABSTRACT

THE EFFECTS OF SKIN-TISSUE MORPHOMETRY ON THE MECHANICAL IMPEDANCE OF RAT GLABROUS SKIN

In this thesis, the mechanical impedance of rat glabrous skin was measured at two different locations: the digit and the sole in the hind paw, at two frequencies: 40 Hz and 250 Hz with amplitude of 61 μm. The force (F), the velocity (v) and the phase difference between them (ϕ) were measured to calculate the mechanical impedance components. Skin samples were also studied histologically from the same locations where the impedance measurements were obtained. On the microscope images, morphometrical measurements of the skin layers were performed. All mechanical impedance and morphometrical measurements were done in two different conditions: the normal and the epidermis-peeled condition.

In the normal condition, two-way ANOVA showed that the effect of the location on the resistance was marginally significant ($p=0.056$), whereas the frequency had no effect ($p=0.376$). The effect of the frequency on the modulus was found to be significant ($p=0.018$); however, the effect of the location on the modulus was not significant ($p=0.684$). In the normal condition, there was a significant correlation between the resistance and the stratum corneum thickness at 40 Hz in the sole and marginally in the digit ($r=0.61$, $p=0.06$ for the digit; $r=0.94$, $p<0.0001$ for the sole). In the peeled condition, at 40 Hz, the remaining epidermis thickness in the digit was significantly correlated with the resistance, the reactance and the modulus ($r=0.91$, $p<0.001$ for the resistance; $r=0.80$, $p<0.01$ for the reactance; $r=0.90$, $p<0.001$ for the modulus). No correlations were found at 250 Hz either on normal and peeled conditions.

According to these results, the impedance was found to be largely governed by resistance. The resistance of the skin was affected by the location and it was highly correlated with the stratum corneum thickness at 40 Hz. This suggests that stratum corneum may determine the mechanical properties of the skin at 40 Hz.

Keywords: mechanical properties of the skin, skin layers, skin histology.

ÖZET

DERİ-DOKU MORFOMETRİSİNİN SIÇAN TÜYSÜZ DERİSİNİN MEKANİK EMPEDANSI ÜZERİNDE ETKİSİ

Bu tez çalışmasında, sıçan tüysüz derisinde iki farklı noktada (parmak ve ayak tabanı) $61\mu m$ genlikli iki farkli frekansta (40 Hz ve 250 Hz) mekanik empedans ölçümleri yapılmıştır. Kuvvet (F), hız (v) ve bunların arasındaki faz farkı (ϕ) mekanik empedans komponentlerini hesaplamak için kaydedilmiştir. Ayrıca mekanik ölçümlerin alındığı noktalardan deri örnekleri deri katmanlarının morfometrik analizi (toplam deri, toplam epidermis, stratum korneum, canlı epidermis ve dermis kalınlıkları) için histolojik olarak incelenmiştir. Bütün mekanik ve morfometrik ölçümler iki farklı koşul altında gerçekleştirilmiştir: normal koşul ve epidermis-sıyrılmış koşul.

Two-way ANOVA sonuçlarına göre, normal koşulda lokasyonun deri direncini az miktarda etkilediği görülmektedir (p=0.056), fakat frekansın bir etkisi görülmemektedir (p=0.376). Frekansın empedans genliği üzerine etkisi istatiksel olarak önemli bulunmuştur (p=0.018), bununla birlikte lokasyonun bir etkisi görülmemiştir (p=0.684). Normal koşulda, 40 Hz'de, parmakda ve ayak tabanında, deri direnci ve stratum korneum kalınlığı arasında istatiksel olarak önemli ve pozitif bir korelasyon vardır (r=0.061, p=0.06 parmak için; r=0.94, p<0.0001 ayak tabanı için). Sıyrılmış koşulda, 40 Hz'de, parmakta, kalan epidermis kalınlığı deri direnci, sıkılığı ve empedans genliği ile önemli ölçüde koreledir (r=0.91, p<0.001 deri direnci için; r=0.80, p<0.01 deri reaktansı için; r=0.90, p<0.001 empedans genliği için). 40 Hz'de, ayak tabanında, kalan epidermis kalınlığı ve mekanik empedans komponentleri arasında istatiksel anlamda önemli bir korelasyon görülmüştür. 250 Hz'de herhangi bir korelasyon mevcut değildir.

Sonuçlara göre, mekanik empedans için deri direnci büyük ölçüde belirleyicidir. Deri direnci 40 Hz'de lokasyondan etkilenmiştir ve deri direnci stratum korneum kalınlığı ile istatiksel anlamda önemli dercede koreledir. Bu duruma göre, stratum korneumun 40 Hz'de derinin mekanik özelliklerini belirlediği düşünülmektedir.

Anahtar sözcükler: derinin mekanik özellikleri, deri katmanları, deri histolojisi.

TABLE OF CONTENTS

LIST OF FIGURES

LIST OF TABLES

LIST OF SYMBOLS

Z	Mechanical impedance
F	Force
v	Velocity
b	Damper constant (resistance)
k	Spring constant (stiffness)
m	Mass
i, j	Imaginary unit
t	Time
w	Angular velocity
m_p	Mass of the contactor and the sensor
ϕ	Phase angle between the force and the velocity

LIST OF ABBREVIATIONS

CNS	Central nervous system
ECM	Extracellular matrix
DAQ	Data acquisition card
LPF	Low-pass filter
NaBr	Sodium bromide
NBF	Neutral buffered formalin
H&E	Hematoxylin and eosin
TT	Total thickness of the skin
TE	Total epidermis
SC	Stratum corneum
VE	Viable epidermis
D	Dermis
IP	Intraperitoneal
SEM	Standard error of the means

1. INTRODUCTION

1.1 Motivation

One of the recurring questions that appears in psychophysical studies of the tactile system is concerned with how mechanical stimulation is transformed before it reaches the mechanoreceptors. That is, are the mechanical characteristics of the skin and the tissue reflected in psychophysical measurements?

In order to understand how vibrations influence tactile sensation, basic knowledge is needed on a number of different physical and biological factors. Response to vibration is shaped by its frequency, intensity, duration and contact point [1, 2]. Apart from such stimulus parameters, skin biomechanics modify the stimulus [3, 4]. From a physical point of view, the hand and the arm can be considered as a mechanical system, composed of a large number of heterogeneous separate masses of various size, nature and design, e.g. different bone structure, muscle groups, skin, sensory organs, held together by different kinds of elastic and viscous tissues.

When the mechanical stimulus is applied on the skin, it spreads through the skin layers and the inner tissue (muscles, bones, etc.) and produces strains and stresses within each structure [1, 3]. These mechanical loads and the resulting stresses and strains on the skin in which the mechanoreceptors embedded in the skin have role in the neural coding of the tactile perception because these several types of mechanoreceptors signal these deformations to the central nervous system (CNS) ultimately resulting in the perception of the object's attributes such as shape or compliance.

There have been a number of studies which have investigated mechanical response of skin-tissue system to vibratory input [5, 6, 7, 8, 9]. Among these studies, Gilmer (1935) reported that the frequency of maximum sensitivity for the finger shifted from around 250 Hz with a probe of either 3 or 6 mm in diameter, up to around 500-900 Hz with a stimulator fabricated from a needle with a tip on the order of 0.5 mm in diameter [10]. In the light of these results, he suggested that the difference of frequency sensitivity may be caused by two types of probe .

Ten different points on the hand were studied in human subjects by Lundström. According to his findings, for instance, at 100 Hz, these ten different points had different impedance values. The central part of the palm had the lowest impedance which was around 7 Ns/m at 100 Hz; however the two distal points had the highest impedance which was about 22 Ns/m. Additionally, while the fingertip had the highest resonance frequency (200 Hz), the hypothenar and the thenar had the lowest resonance frequency (100 Hz and 110 Hz, respectively) [5].

Additionally, when measurements were made on an area directly over a rib, the results were different from those measurements made on the thigh and the upper arm. Although the resonant frequency of chest was about 600 Hz, the resonant frequency of the thigh was 20 to 30 Hz [9]. The much higher resonant frequency was due to the stiffer structure underlying the body surface in the chest area. These results strongly imply that changes in gross anatomy may affect the mechanical behavior of the skin.

Another study was reported by Weitz in 1939. He was concerned with influence of anaesthesia on tactile perception and noted that when an anesthetized area was stimulated, the resulting behavior of skin was grossly different. Surface disturbance in anesthetized region was much greater than normal skin. In other words, while in the anesthetized area the affected region vibrated as a unit, in the normal skin, this surface disturbance traveled in all directions like ripples [11]. Similar effects were noted by Gilmer when a calloused area of skin was stimulated.

Mann and Griffin studied the effect of the location of contact with the finger in human subjects. They stimulated 6 different points on the finger: the tip of the finger, the center of the distal phalanx, the distal interphalangeal joint, the center of the middle phalanx, the proximal interphalangeal joint and the center of the proximal phalanx. According to their results, the peak values of the modulus of the impedance occured at decreasing frequencies as the location stimulated moved proximally. The maximum impedance was at the fingertip and it was 11 Ns/m, occuring at approximately 600 Hz, whereas the maximum impedance at the center of the middle phalanx was 11 Ns/m at 60 Hz [12].

Wang and Hayward tested the mechanical properties of the fingerpad glabrous skin in humans in vivo under tangential loading. Their results showed that glabrous skin exhibited nonlinear stiffening in tangential traction. The skin was more elastic

across the ridges than along the ridges regardless the location of the sample on the skin [13].

Different from the mechanical impedance measurements, by using streching and shearing tests, Pan et al. found Young's modulus of human forearm skin in vivo, strained at 40%, to be 458.7 kPa [14]. However, Wang and Hayward found Young's modulus of the fingerpad to be 3.61 MPa for along the ridges and 1.54 MPa for across the ridges by strecthing with tangential load [13]. This discrepancy with these two results can be explained by the fact that the stratum corneum of the glabrous skin is at least four times thicker than of that of the hairy skin [15].

Furthermore, Güçlü and Bolanowski (2005) found that the mechanical impedance of the skin is not constant along the proximo-distal axis of the fingertip. This non-uniform distribution of mechanical impedance can be attributed to heterogeneous properties of the skin. Non-uniform mechanical impedance distribution implies the change of stiffness and resistance of skin through the finger [16]. Similarly, Devecioglu showed that along the proximo-distal axis in glabrous skin of rat middle digit, different points have different mechanical impedance values [17].

1.2 Objectives

Following hypotheses were tested in the thesis presented here:

- The mechanical impedance components (the resistance, the reactance and the modulus of the impedance) are affected by the frequency of the stimulus and the location stimulated.
- The morphometrical parameters (the thickness of the skin layers) are different in the digit and the sole.
- The thicknesses of various skin layers are correlated with the mechanical impedance components.

1.3 Outline

The thesis is presented as follows: In chapter 2, background information about the morphology and the structure of the skin layers and skin mechanics is given. In chapter 3, the experimental procedures are explained. In chapter 4, the results are presented. In chapter 5, the discussion of the results and their implications are given.

2. BACKGROUND

Skin is the largest organ of body and the fundamental component of the integumentary system. It makes up 16% of body weight with a surface area of between 1.5-2 m^2 in human. Because of the fact that it interfaces with the environment, skin has several important functions. The main functions are forming a physical barrier to the environment, allowing and limiting the inward and the outward passage of water, electrolytes and various substances and providing protection against microorganisms, ultraviolet radiation, toxic agents and mechanical damage [18]. Furthermore, more importantly, the skin has a key role for the mediation of the tactile sensation via the several types of the mechanoreceptive fibers.

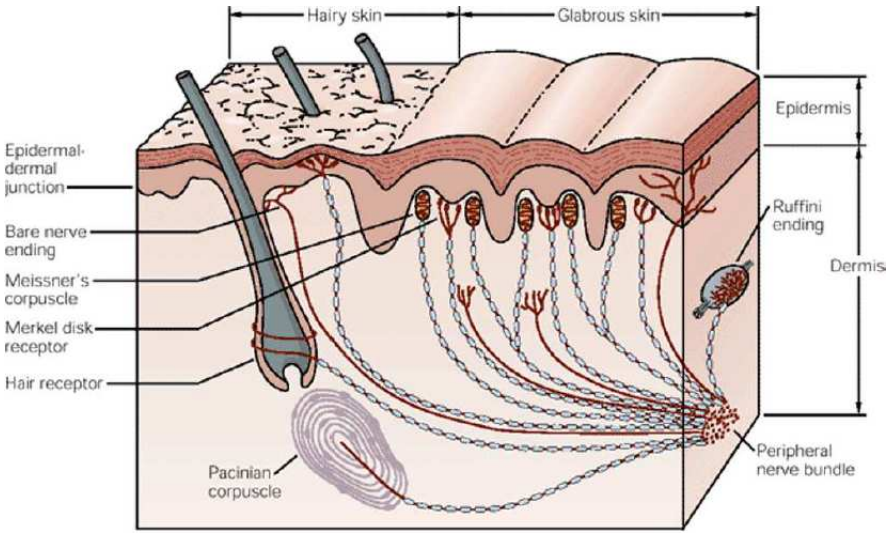

Figure 2.1 An illustration of human glabrous and hairy skin structure [19].

There are three types of skin: glabrous skin, hairy skin and mucocutaneous skin. Glabrous skin is also known as hairless skin and is found on the palms and the soles. It does not contain any hair follicles or sebaceous glands. It is characterized by a thick epidermis and compact stratum corneum and by the presence of encapsulated sense organs within the dermis. Hairy skin has hair follicles and sebaceous glands. There is no encapsulated sense organ in hairy skin except Pacinian's corpuscle [19]. Figure

2.1 shows the structure of human glabrous skin and hairy skin. Mucocutaneous skin is found on lips and nostrils.

2.1 Anatomy of the Glabrous Skin

In general, mammalian skin is composed of three layers; epidermis, dermis and hypodermis (see Figure 2.2).

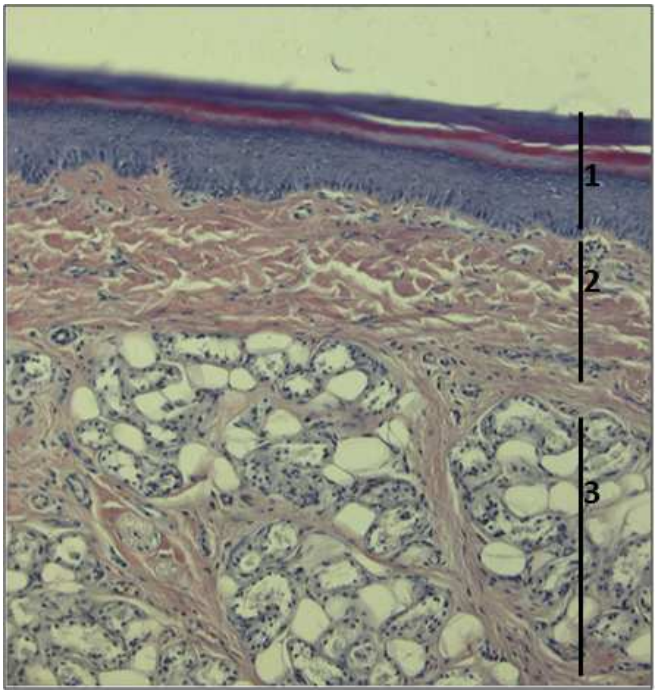

Figure 2.2 The layers of the glabrous skin. Microphotograph of rat glabrous skin from the digit (H&E staining, magnification X40), 1: Epidermis, 2: Dermis, 3: Hypodermis.

2.1.1 Epidermis

It is the first layer of the skin and it consists of keratinocytes which change in cellular constituents as they move peripherally. Several well-defined layers results from this movement of keratinocytes. Epidermis has mainly five layers as shown in Figure 2.3. The deepest layer is the stratum basale and it is also known as the stra-

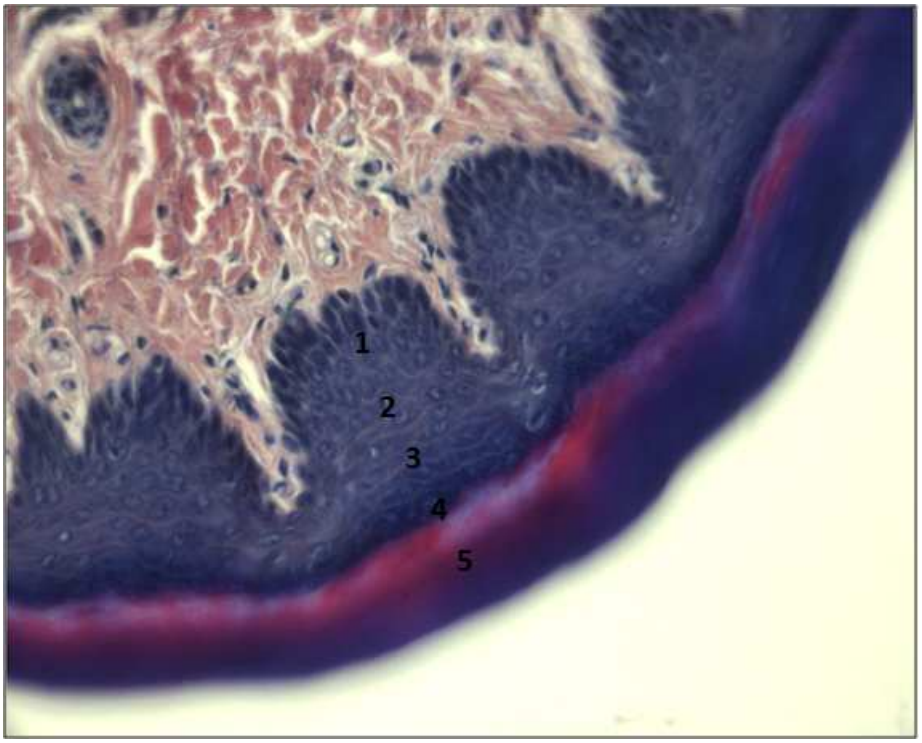

Figure 2.3 The layers of the epidermis. 1: stratum basale, 2: stratum spinosum, 3: stratum granulosum, 4: stratum lucidum, 5: stratum corneum. Microphotograph of rat glabrous skin from the digit (H&E staining, magnification X40).

tum germanitivum. Cell division occurs in this layer. It consists of 1-3 layers of small cuboidal cells with large nuclei and cytoplasm. As the cells move towards the surface, they become larger and they form the stratum spinosum. The polyhedral cells of the stratum spinosum are connected by desmosomes. Their shape becomes more flattened as they move outward. In the stratum granulosum the degradation of mitochondria and nuclei starts and the cytoplasm of the flattened cells become almost filled by keratohyalin masses and filaments. Also the cell membranes become gradually thicker. These three layers; stratum basale, stratum spinosum and stratum granulosum, are also called viable epidermis because the cells are still alive in these layers [20]. The stratum lucidum is located between stratum granulosum and stratum corneum and composed of a few dead and flattened keratinocytes. It is not a clearly discriminable layer [20, 21]. The most superficial layer, the stratum corneum consists of 15-20 layers of dead a nucleate cells that are hexagonal thin flat squames. At this stage the cells are terminally differentiated keratinocytes which are called corneocytes [20].

• **Stratum Corneum**

Stratum corneum is the top layer of the epidermis. It is composed of hexagonal flat cells without a nucleus called corneocytes, held together by lipids and desmosomes in what is commonly referred to as a brick-and-mortar structure (Figure 2.4).

The diameter and the thickness of corneocytes range from 25-45μm and approximately 0.3-0.7 μm, respectively [22, 23]. In human skin, the stratum corneum consists of 15-25 [23, 24] layers of corneocytes, resulting in a total layer thickness of about 10-25μm [25]. The lipids are arranged in lamellar sheets, which consist of membrane-like bilayers of ceramides, cholesterol, and fatty acids together with small amounts of phospholipids and glucosylceramides. The intercellular spaces, i.e. the distance between neighboring corneocytes, are about 0.1-0.3μm [26]. Desmosomes, also called corneosomes, are specialized inter-corneocyte linkages formed by proteins and, together with the lipids, they keep the integrity of the stratum corneum [27]. The lipids form the major permeability barrier to the loss of water from the underlying epidermis.

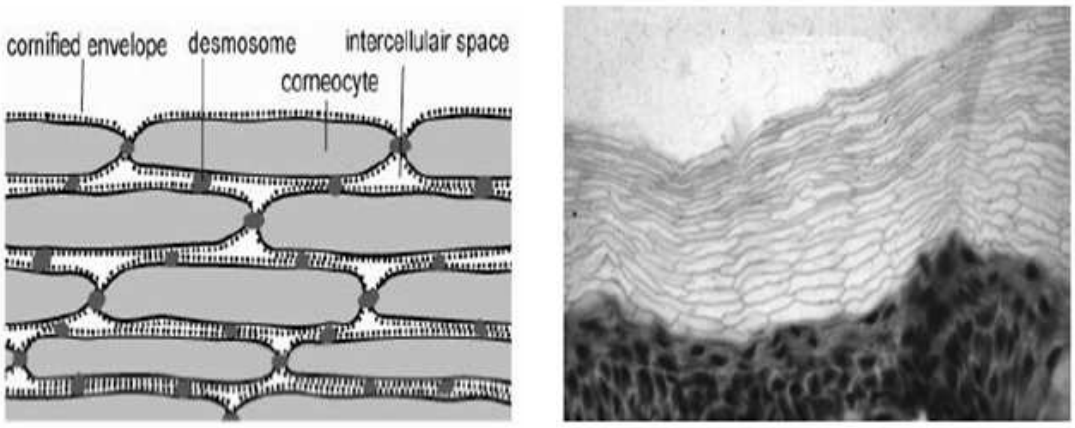

(a) (b)

Figure 2.4 Morphology of the stratum corneum. (a) Schematic drawing (b) cryostat section of normal human skin treated with Sorensen's alkaline buffer and methylene blue [22].

The stratum corneum, and viable epidermis, is continuously renewed within 6 to 30 days in human skin [28]. Cells are shed from the outside and replaced by new ones. Changes in structure, composition and function of the corneocytes occur as they

move toward the outer skin surface. Cells of the deeper layers of the stratum corneum are thicker and have more densely packed arrays of keratins, a more fragile cornified cell envelope and a greater variety of modifications for cell attachment. Consequently, the deeper part of the stratum corneum has a major influence on its overall mechanical behavior. The outer stratum corneum cells have less capacity to bind water. The cells in the outermost stratum corneum have a rigid cornified envelope and in the same area, the desmosomes undergo proteolytic degradation.

Although the corneocytes are non-viable, the stratum corneum is considered to be fully functional, particularly in terms of barrier properties, and retains metabolic functions [29].

- **Viable Epidermis**

The viable epidermis is a layered structure. It consists of three layers, stratum basale, stratum spinosum and stratum granulosum. Most of the epidermal cells are the keratinocytes. They migrate upwards to the skin surface where they become non-viable and more flattened. Other cell types within the viable epidermis include melanocytes, Langerhans cells and Merkel cells [20].

Keratinocytes change their shape, size and physical properties when migrating to the skin surface. Indeed the morphology of an individual keratinocyte correlates with its position within the epidermis and its state of differentiation, which is reflected by the different strata: the stratum basale, the stratum spinosum and the stratum granulosum. The deepest layer is the stratum basale in which cell division occurs. It consists of 1 to 3 layers of small cubic cells. In the next layer, the stratum spinosum, the cells are larger and polyhedral in nature and are connected by desmosomes, which are symmetrical laminated structures. The keratinocytes adopt a more flattened morphology at higher layers of the stratum spinosum. In this layer, they are associated with lamellar granules, which are lipid-synthesizing organelles that migrate toward the periphery of the cell and eventually become extruded into the intercellular compartment in the next layer, the stratum granulosum. At this stage of differentiation, the degradation of mitochondria and nuclei is apparent and the cytoplasms of the flattened cells become increasingly filled with keratohyalin masses and filaments. Furthermore, the cell membrane becomes

gradually thicker [19, 20, 21].

In the human skin, the thickness of the viable epidermis varies roughly between 30-100μm [30], accomodating between 5 to 10 cell layers. The cells are communicating by very strong desmosomes in the very compact tissue; the intercellular spaces occupy less than 2% of the volume [25, 31]. Therefore, the mechanical integrity of the viable epidermis is considered to be stronger than other soft tissues.

Because of its non-vascular structure, the epidermal cells are nourished from plasma that originates in the dermal blood vessels such that the nutrients transport across the epidermal-dermal junction.

2.1.2 Dermis

The dermis makes up most of the human skin and contributes to 15-20% of the total body weight. It contains a lot of irregularities such as blood vessels, lymph vessels, nerve endings, sebaceous glands and sweat glands (Figure 2.5). Also it contains mast cells, macrophages, lymphocytes and dermal dendrocytes. The dermis is a moderately dense connective tissue which consists of three fibrin proteins, namely collagen, elastin and minute quantities of reticulin and a supporting matrix or ground substance. Collagen comprises about 75% of the fat free dry weight and 18-30% of the volume of dermis [32].

Finlay (1969) showed that the collagen fibre bundles form an irregular network that runs almost parallel to the epidermal surface [33]. Interwoven among the bundles of collagen, is a network of elastin that restores the normal fibrous array following its deformation by external mechanical forces. These elastic fibres contribute to 4% of the fat free dry weight and 1% of the volume of dermis [32]. According to Oxlund et al. (1988) direct connections between elastin and collagen fibres have not been shown, but collagen fibrils appear to wind around the elastin cores [34]. At extension rates of about 1.3, the undulated collagen fibrils are straightened. The amorphous ground substance is composed of glycosaminoglycans, long chains of polysaccharides, which are able to bind a high amount of water. Together they form a gel which does not leak out of the dermis, even under high pressure.

The dermis is arbitrarily divided into two anatomical regions: the papillary dermis and the reticular dermis. The papillary dermis is the thinner outermost portion of the dermal connective tissue, constituting approximately 10% of the thickness of the dermis. It contains smaller and more loosely distributed elastic and collagen fibrils than the underlying reticular dermis and it has a greater amount of ground substance. The reticular dermis constitutes the greater bulk of the dermis. This dense collageneous and elastic connective tissue contains a relatively small amount of cells and veins [32].

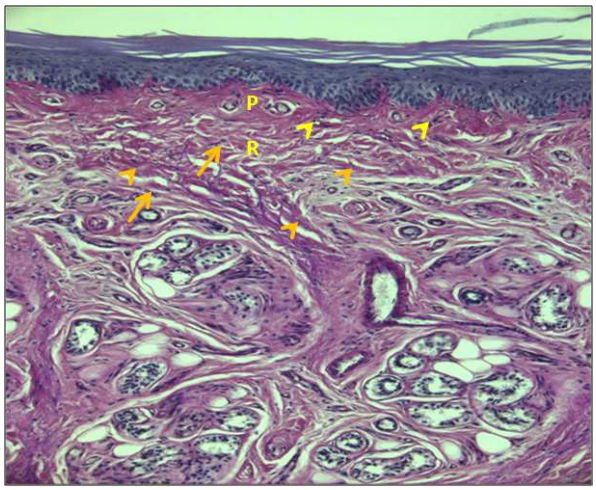

(a)

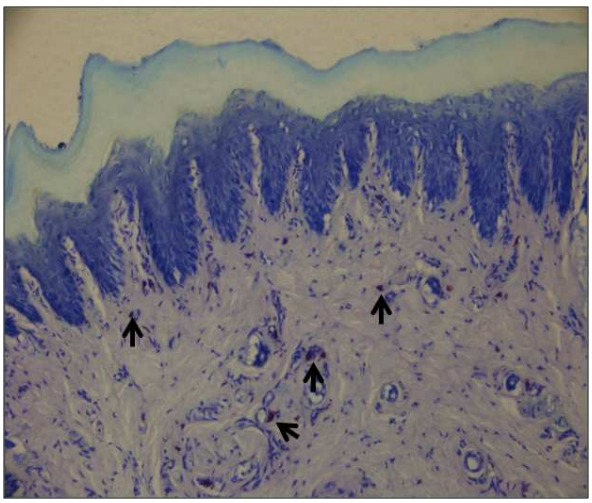

(b)

Figure 2.5 Morphology of Dermis. (a) Microphotograph of rat glabrous skin with Periodic Acid and Schiff Base staining (PAS) (P: Papillary dermis, R: Reticular dermis, Orange arrows indicate elastin fibers, Orange arrowheads indicate collagen fibers,Yellow arrowheads indicate fibrinocytes. Magnification X20) (b) Microphotograph of rat glabrous skin with Toluidine-Blue staining (Black arrow show mast cells. Magnification X20)

2.1.3 Hypodermis

The hypodermis is defined as the adipose tissue layer found between the dermis and the aponeurosis and fasciae of the muscles. Its thickness varies with anatomical site, age, sex, race, endocrine and nutritional status of the individual. The subcutaneous adipose tissue is structurally and functionally well integrated with the dermis through nerve and vascular networks and the continuity of epidermal appendages, such as hairs and nerve endings.

The bulk of subcutaneous adipose tissue is a loose association of lipid-filled cells, the white adipocytes, which are held in a framework of collagen fibers. However, only one third of adipose tissue contains mature adipocytes [35].

2.2 Skin Mechanics

An important function of the glabrous skin is to mediate tactile sensations. When one touches an object, mechanical loading causes the skin to deform from a relaxed state. Several types of mechanoreceptors which are embedded in the skin signal these deformations to the central nervous system (CNS), ultimately resulting in the perception of the object's attributes such as shape or compliance. A characterization of the biomechanics of the glabrous skin would contribute to the understanding of the tactile function since receptors respond to patterns of skin deformation. The anisotropic material properties which cause different strain patterns might account for directionality of the tactile afferent fibers [36]. The tactile perception also affected by the viscoelasticity of the skin [37].

Mechanical properties of the skin have been investigated by using different techniques. For instance, from 1970's, various authors have reported tensile results [25, 38, 39, 40, 41]. Subsequently, torsional techniques were developed to measure the stratum corneum behavior in vivo [42, 43, 44, 45]. More recently, indentation techniques were introduced to determine the Young's modulus in vitro and also in vivo indentation tests have been performed. Furthermore, imaging techniques such as ultrasound and magnetic resonance elastography have been used to estimate mechanical

properties [46]. Reported Young's moduli vary considerably encompassing values from a few MPa to GPa [38, 39]. Current constitutive models of the stratum corneum are based on traction, relaxation and creep tests [25].

In the literature, a limited number of studies are available regarding the mechanical behavior of the viable epidermis and the hypodermis. From an indentation approach, a local Young's modulus of a few MPa has been reported for the viable epidermis of murine ear skin [47, 48]. The mechanical behavior of subcutaneous adipose tissue in hypodermis was subjected to shear and compression test [49] and Young's moduli vary from a few kPa to values more than of 100 kPa.

Contribution of the extracellular matrix which is composed of a variety of polysacharides, water, collagen, elastin and reticulin to mechanical properties of the skin cannot be ignored. The ECM determines the mechanical properties of the skin and gives it the unique properties of elasticity, compressibility and tensile strength [13]. Collagen fibres are the major constituent of dermis and form an irregular network of wavy coiled fibres that run almost parallel with the skin surface [35]. Collagen fibres are characterized by high stiffness. Young's modulus of collagen fibres is approximately from 0.1 GPa [50] to 1 GPa [51]. Elastin fibres are the second major components of dermis. They are less stiff and more extensible than collagen fibers. Elastin fibers provide the skin with high deformability. They can be reversibly stretched to more than 100% [52]. Thus, elastin fibers support the recovery of the skin shape by acting as a spring. Reticulin is found much smaller amounts. Mechanical properties of reticulin are not clearly known. Proteoglycans in ECM contribute to the viscosity of the skin because they play a role during displacement of interstitial fluid and interact with collagen fibres [53].

Güçlü and Bolanowski (2005) showed that the mechanical impedance of the skin is not constant along proximo-distal axis [16]. The anisotropic property of the skin causes this non-uniform distribution of the mechanical impedance. Non-uniform distribution of the mechanical impedance implies changes in the stiffness and the resistance of the skin through the body.

The mechanical impedance of the skin (Z) is the complex ratio of F and v. In other words, Z can be expressed in terms of the force (F) and the velocity (v) applied

to the skin together with the phase difference between F and v (ϕ) (Eq. 2.1).

$$Z = \frac{F}{v} \tag{2.1}$$

where

$$F = F_0 e^{iwt}, \quad v = v_0 e^{i(wt-\phi)} \tag{2.2}$$

Eq. 2.1 enables us to express Z in terms of the resistance and the reactance as in Eq 2.3. It may be divided into real and imaginary components.

$$Z = Re\{Z\} + jIm\{Z\} \tag{2.3}$$

Where $Re\{\mathrm{Z}\}$ is the resistance of the mechanical impedance,$Im\{\mathrm{Z}\}$ is the reactance of the mechanical impedance. Resistance results from energy dissipation in the system. Reactance results from the storage of either kinetic or elastic energy, which is released in another phase of the time varying cycle [8].

3. MATERIALS AND METHODS

3.1 Animals

The experiments were approved by Boğaziçi University Institutional Ethics Committee for the Local Use of Animals in Experiments. 10 adult Wistar albino rats of either sex (5 males and 5 females), randomly selected, 4-5 months old, from the university vivarium were used in this study. They were held in cages and maintained on a 12-h light/12-h dark cycle in a ventilated vivarium (21±2 °C). Food and water were available *ad libitum*.

3.2 Mechanical Impedance Measurement Procedure

3.2.1 Apparatus

The block diagram of mechanical impedance measurement setup is shown in Figure 3.1. A custom-made MATLAB (The MathWorks, R2008a) code was used to generate the stimulus pattern and the amplitude of the stimulus was controlled by the software. The data acquisition card (DAQ) (National Instruments) was used to convert the digital stimulus pattern coming from MATLAB into an analog signal. A custom made low pass filter (LPF) was used to filter high frequency switching noise in the stimulus signal. In order to adjust the amplitude of the stimulus, a digital attenuator (ISR Active Attenuator) was used. A custom-made power amplifier was used to drive the shaker (Ling Dynamic System V101). The shaker was mounted on a custom-made structure and a boom stand. It could be positioned in all three axes and lowered onto the skin. A delrin probe (0.74 mm in diameter) was used to stimulate the skin. A Type 8001 (Brüel and Kjaer) impedance head was used to measure the mechanical impedance of the skin. A Nexus Type 2692 conditioning amplifier (Brüel and Kjaer) was used to filter, amplify and calibrate the acceleration and the force signals from the

impedance head. The acceleration signal from the impedance head was integrated by the conditioning amplifier to obtain the velocity signal. The velocity and the force signals from conditioning amplifier were measured on the digital oscilloscope (Tektronix) screen.

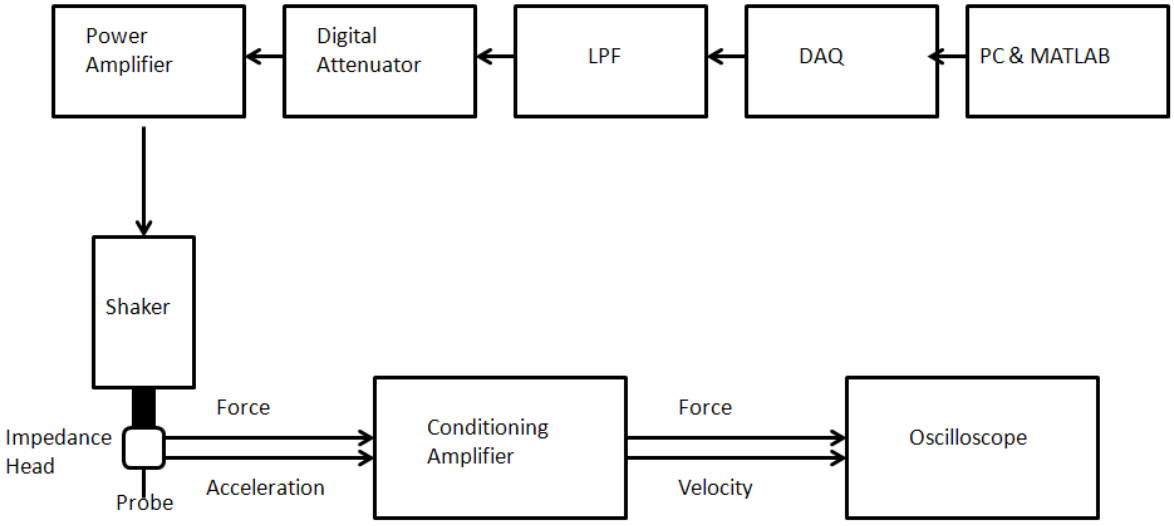

Figure 3.1 Block diagram of the mechanical impedance measurement set up, modified from Devecioğlu [17].

3.2.2 Animal Preparation

The mechanical impedance measurements were done on anesthetized animals. The animals were first anesthetized with an induction dose of 65 mg/kg ketamine and 10 mg/kg xylazine intraperitoneally (IP). Supplementary doses (1/3 of induction dose) were given as required. After the rat was placed on the experiment table, its rectal temperature, respiration rate, and pedal reflexes were monitored. Body temperature was kept at 37 °C by the heating pad. The right hind paw was fixed with modelling clay; glabrous skin was facing up.

After the measurements were completed, animals were perfused transcardiacally and the right and the left hind paws were collected for histology work and morphometrical analysis.

3.2.3 Mechanical Stimulation and Mechanical Impedance Measurement

The mechanical impedance measurement procedure and set up are given in Figure 3.2 and Figure 3.3, respectively. Two different sites on the right hind paw of were chosen for all impedance measurements. These sites were the digit and the sole. Probe was placed on the middle point of the digit. For the sole, probe was placed on a predefined point above the heel (see Figure 3.4 for detailed information).

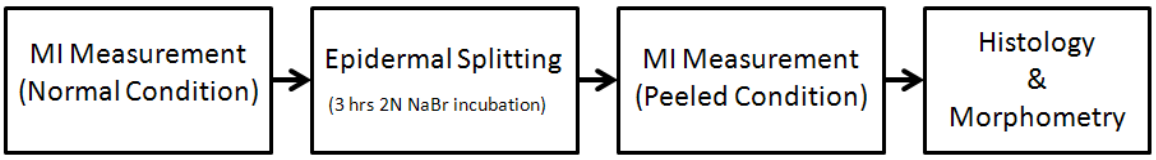

Figure 3.2 Block diagram of the procedure.

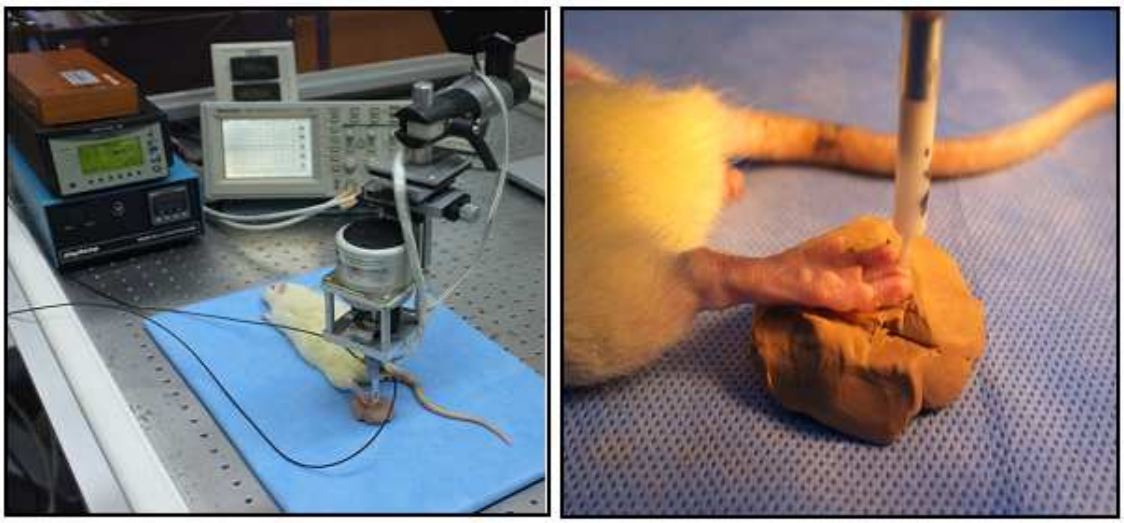

Figure 3.3 Mechanical impedance measurement set-up.

The mechanical impedance measurements were done under two conditions: the normal condition and the peeled condition which the epidermis of the glabrous skin was partially or completely removed by sodium bromide (NaBr) incubation method. After the mechanical impedance was measured in the normal condition, the right hind paw of rat was immersed in 2M aqueous solution of NaBr for 3 hours in order to peel

the epidermis off. After the incubation, the epidermis was removed gently with fine forceps [54, 55].

Sinusoidal mechanical vibrations at frequencies of 40 Hz and 250 Hz with amplitude of 61 μm were applied perpendicular to the hind paw glabrous skin. The duration of stimulus was 2 minutes. The glabrous skin of the digit and the sole was stimulated with one contactor size (diameter of contactor: 0.74 mm). 0.5-mm pre-indentation was used to prevent decoupling of the contactor and the skin.

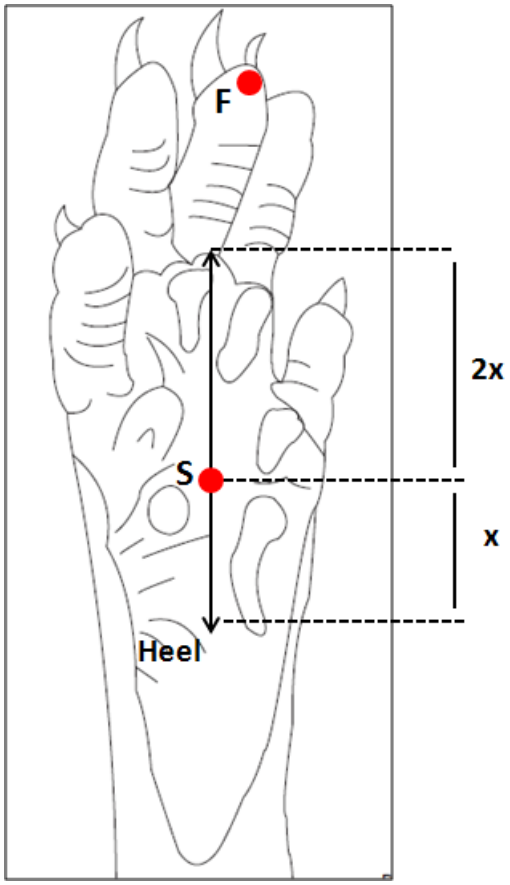

Figure 3.4 Approximate stimulation sites.

The velocity (v) and the force (F) values from the conditioning amplifier were recorded for each location and frequency at 4 repetitions. The complex ratio of F to v gives the mechanical impedance (Eq 3.1). The mechanical impedance has real and imaginary components. Damping produces the real component, also known as the mechanical resistance ($Re\{\mathrm{Z}\}$). The mechanical resistance was calculated by using Eq 3.2. The mass and the stiffness produce the imaginary component ($Im\{\mathrm{Z}\}$), also known as

the mechanical reactance. During the calculation of the reactance, mass compensation was done by using Eq 3.3.

$$Z = \frac{F}{v} \tag{3.1}$$

$$Resistance = Re\{Z\} \tag{3.2}$$

$$Reactance = Im\{Z\} - m_p\omega, \qquad m_p = mass\ of\ the\ contactor\ and\ the\ sensor \tag{3.3}$$

$$Modulus = |Z| \tag{3.4}$$

3.3 Histology

3.3.1 Apparatus and Chemicals

- **Apparatus**

The automated tissue processing machine (Leica TP-1020, Germany) was used in tissue processing step. Paraffin embedding was done by using tissue embedding system (Leica EG1150H and Leica EG1150C, Germany). A fully automated rotary microtome (Leica RM2255, Germany) was used for sectioning step. For tissue sectioning, microtome blade (Feather N35, Japan) was selected based on the tissue type. An incubator (Nuve EN-025,Turkey) was used for the recovery of the skin samples.

- **Chemicals**

Formaldehyde, the absolute ethanol, paraffin and entellan (the mounting media) was purchased from Merck Millipore, USA. The absolute ethanol was diluted by

distilled water based on the protocol. Xylene (Sigma-Aldrich, Germany) was used as a clearing agent.

3.3.2 Tissue Collection and Fixation

Following the completion of the mechanical impedance measurements, the glabrous skin samples from stimulation sites on the digit and the sole were collected from the transcardiacally perfused animal. The digit and the sole samples from the left hind paw were collected as a control in order to compare the morphology of the skin in the normal and the peeled condition.

The length of the digit were measured with electronic calipers before and after splitting of the epidermis. In the sectioning part of the histology, the skin samples selected for morphometrical analysis from intact and peeled skin must be from approximately same point to compare the thickness of the skin layer before and after peeling. Hence, the differences in length before and after peeling of epidermis is crucial for determination of skin samples in right depth during sectioning step.

Tissues were stored in 10% neutral buffered formalin (NBF; 10% formaldehyde in phosphate buffered saline) for four days to improve fixation. Fixation is needed to preserve biological material as close to natural state as possible by stopping postmortem decay (autolysis and putrefaction) in tissue cells.

3.3.3 Tissue Processing

After tissue collection and fixation, tissue processing was performed. Tissue processing involved the following steps (see table 3.1 for detailed information);

- **Dehydration:** Water is the main constituent of the biological tissues. It must first be removed form the tissue because usually, embedding media cannot directly replace water. The most used dehydrating agents are ethanol and acetone.
- **Clearing:** Solidifying agents (paraffin wax, agar or gelatine) cannot replace

with the water. Therefore, a clearing step is needed to replace water with xylene.

- **Infiltration:** This is the final step of the tissue processing. Paraffin was used as a solidifying agent. Molten paraffin replaces xylene and it hardens the tissue. Hardening of tissue is needed for good sectioning.

Table 3.1
Tissue processing protocol, 1: Dehydration, 2: Clearing, 3: Infiltration.

Steps	Chemicals	Duration
1	70% Ethanol	1-h
	80% Ethanol	1-h
	80% Ethanol	1-h
	96% Ethanol	1-h
	96% Ethanol	1-h
	100% Ethanol	1-h
	100% Ethanol	1-h
2	Xylene	1-h
	Xylene	1-h
3	Paraffin	1-h
	Paraffin	1-h

3.3.4 Paraffin Embedding and Tissue Sectioning

During this step, the tissue samples were placed into molds along with liquid embedding material (such as agar, gelatine or paraffin wax) which is then hardened. This is achieved by cooling in the case of paraffin wax. NBF-fixed, paraffin-embedded tissues may be stored for a long time at room temperature. Paraffin embedding was performed with heated paraffin embedding machine. Cold plate for modular tissue embedding system was held at a constant temperature of $-5°C$ to provide rapid cooling of the embedded blocks and molds. Tissue samples were placed into embedding casettes

in order to make them appropriate for sectioning in microtome.

Fully automated rotary microtome was used for taking 10 μm thick tissue sections. These sections were moved to a water bath (45°C) and were placed on glass slides. Then, they were placed in an incubator overnight at 37°C in order to get rid of the remaining paraffin and to recover the tissue. During tissue sectioning, the sections were selected for morphometry according to specific plan. Based on the contactor size (0.74 mm in diameter), five different sections were chosen near the mechanically stimulated point. The distance between each selected section was 100 μm (Figure 3.5).

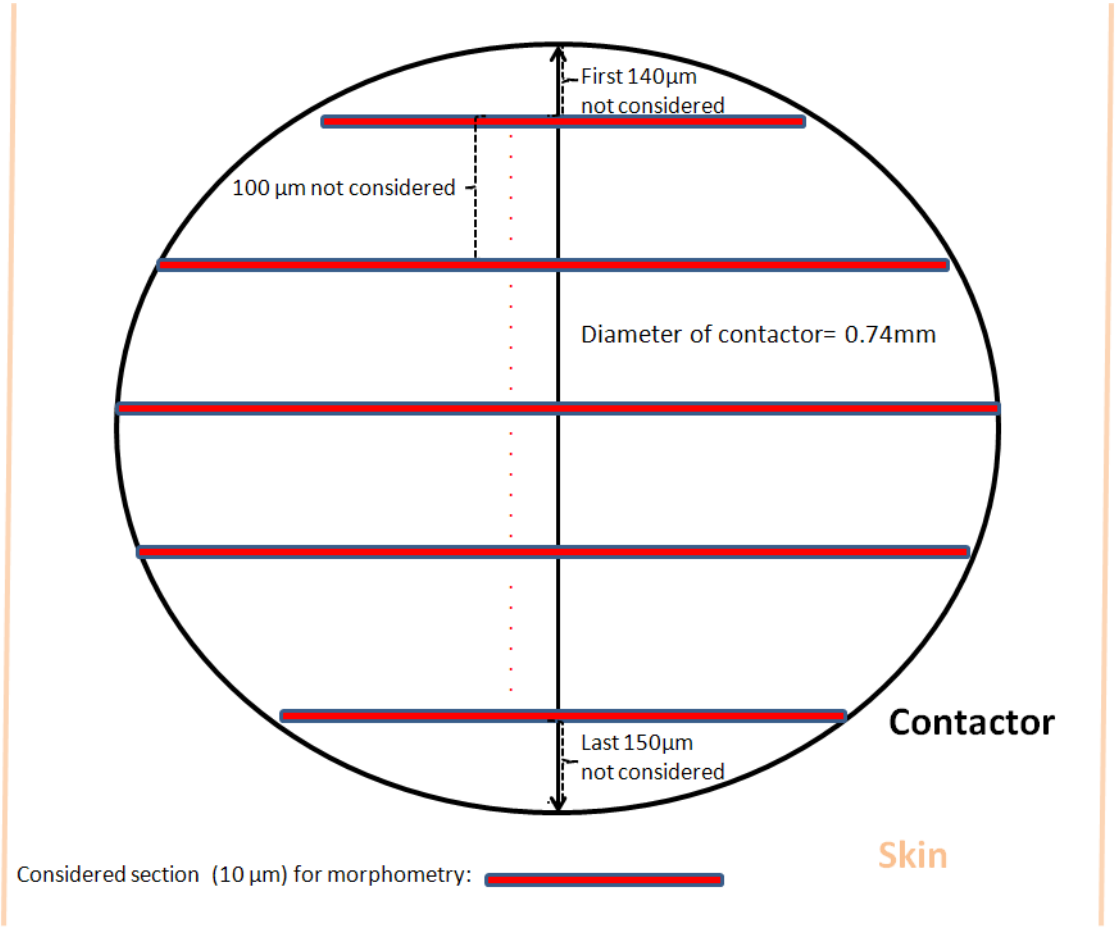

Figure 3.5 Criteria for choosing skin samples during sectioning for histology.

3.3.5 Tissue Staining

Staining is employed to give both contrast to tissue as well as highlighting particular features of interest. Hematoxylin and eosin (H&E) staining was used for histological examinations. This combined stain gives information about the gross anatomy of the tissue. Hematoxylin, a basic dye, stains the nuclei blue due to an affinity to nucleic acids in the cell nucleus; eosin, an acidic dye, stains the cytoplasm, reticular and elastic fibers pink [56, 57].

In the first step, incubated slides were placed into xylene for 5 minutes in order to remove of paraffin from the tissue. Then, slides were sequencially dipped in absolute alcohol and 90% alcohol for 10 times for rehydration. Afterwards, slides were washed with tap water and were placed into hematoxylin for 90 seconds. Hematoxylin is a progressive dye, hence the duration of hematoxylin application had adjusted carefully.

In order to remove the excessive stain, slides were then dipped in 90% alcohol for 10 times. Slides were put into eosin for 2 minutes for counterstaining. Then, slides were dipped into 90% and absolute alcohol for 10 times for dehydration and to remove excessive eosin, respectively. Xylene was used in the final step of staining as a clearing agent. The duration of xylene application was approximately a few minutes. After clearing, entellan, a xylene based mounting media, was applied the tissue and glass coverslip was placed.

3.4 Morphometrical Analysis

After completion of all histology procedures, the following parameters (see in Figure 3.6) were considered in the morphometrical analysis of skin layers;

- Total thickness of the skin (TT) (calculated)
- Total Epidermis thickness (TE) (measured)
- Stratum corneum thickness (SC) (measured)
- Viable Epidermis thickness (VE) (calculated)
- Dermis thickness (D) (measured)

All measurements were done by using Leica DM2000 microscope and Leica imaging software (LAS). The total epidermis, stratum corneum and dermis thicknesses were measured at 5 different points. Then the viable epidermis thickness was calculated by substracting the stratum corneum thickness from the total epidermis thickness. Again, specific methodology was used in order to standardize the morphometrical measurements. At first, the mid-point of the sample was determined and, then, from the middle of the sample to both left and right direction by 150 μm intervals, two different points were chosen (Figure 3.7). All parameters were measured at these 5 different points.

3.5 Statistical Analysis

MATLAB was used for statistical analysis. Two-way ANOVA was used to test any significant effects of frequency and location on the mechanical impedance measurements in the intact skin and the peeled skin. Paired t-test was used to test the hypothesis that the thickness of the glabrous skin layers are different in the fingertip and the sole in intact skin. In addition, paired t-test was used to test whether epidermis was significantly peeled after the NaBr incubation or not. The correlation tests were done to show whether there was any significant correlation between the morphometrical data and the mechanical impedance measurements.

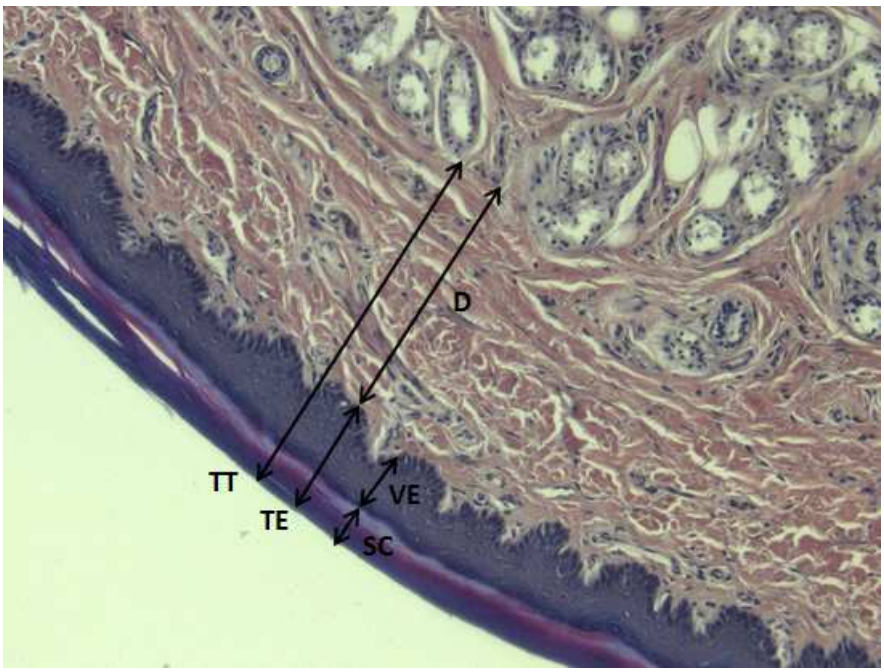

Figure 3.6 Parameters used in morphometrical analysis.

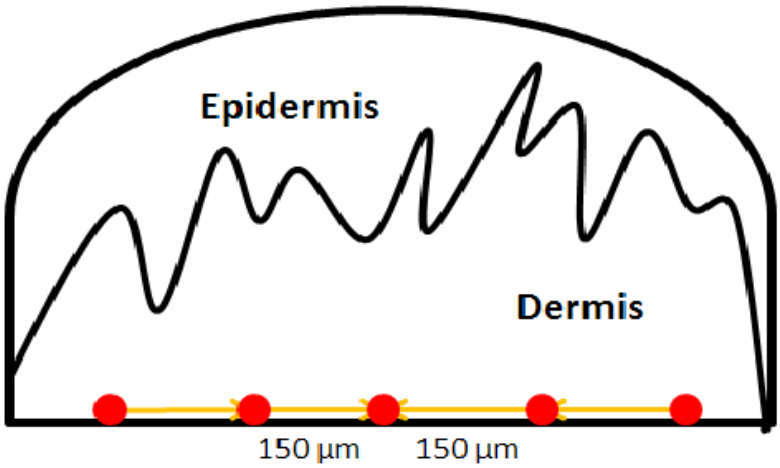

Figure 3.7 Fiducial points used in morphometrical analysis to measure the thickness of the skin layers: Red dots show the points.

4. RESULTS

4.1 Skin Morphometry

Two sites, digit and sole, were studied for morphometrical analysis (Figure 4.1). Total epidermis thickness (TE), stratum corneum thickness (SC) and dermis thickness (D) were measured. Total thickness of skin (TT) and viable epidermis thickness (VE) were calculated.

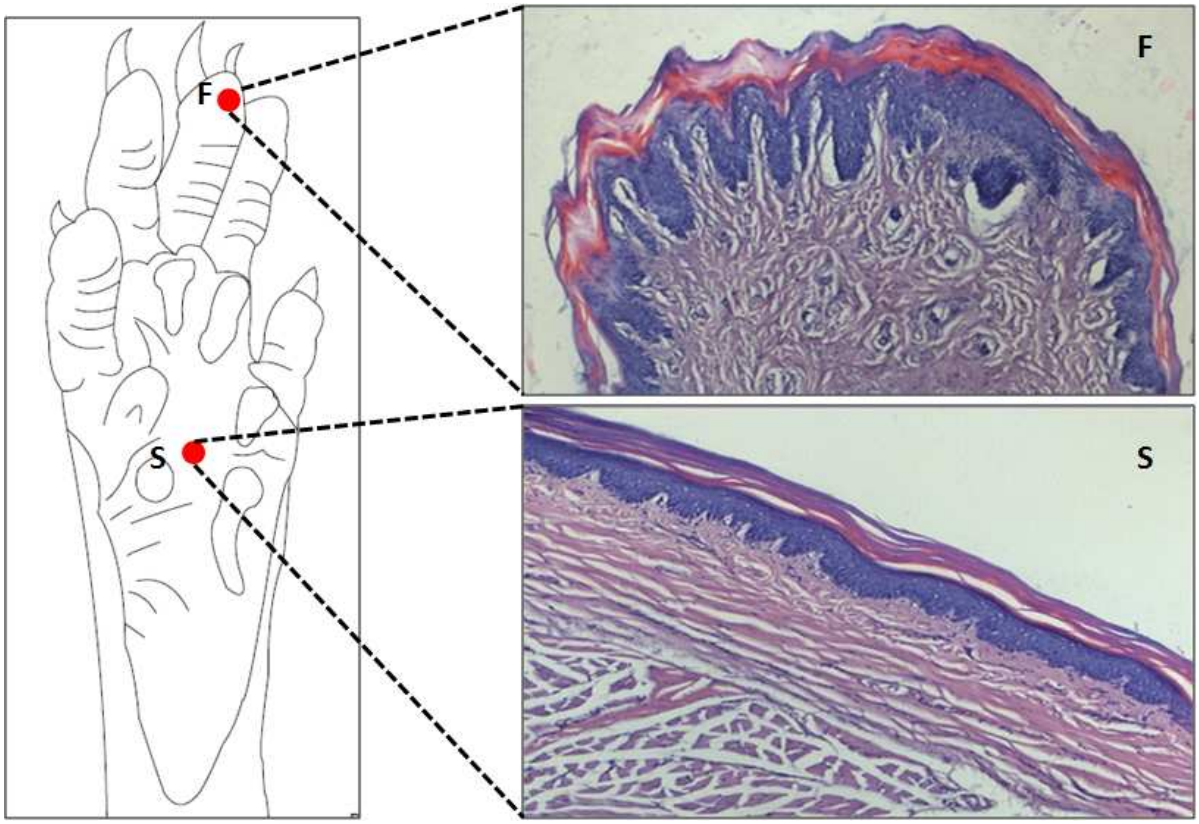

Figure 4.1 Anatomy of glabrous skin in the digit and the sole.

As shown in Table 4.1 and Figure 4.2, the thickness of all meausured skin layers in fingertip is greater than the thickness of the corresponding layer in the sole and the distinct in thickness of each skin layers between fingertip and sole is statistically significant (see p-values in Table 4.1, Two-way ANOVA). For instance, while total skin

thickness is about 683μm±43.06, total skin thickness in sole is about 343μm±25.79.

Table 4.1
Location dependent changes in the thickness of the skin layers.

Location	TT(μm)	TE(μm)	SC(μm)	VE(μm)	D(μm)
Digit	683.08±43.06	186.41±25.53	77.06±11.52	109.35±18.96	496.67±45.69
Sole	343.27±25.79	117.47±11.20	54.78±6.85	63.19±12.44	225.80±22.07
p-value	<0.0001	<0.0001	<0.0001	<0.001	<0.0001

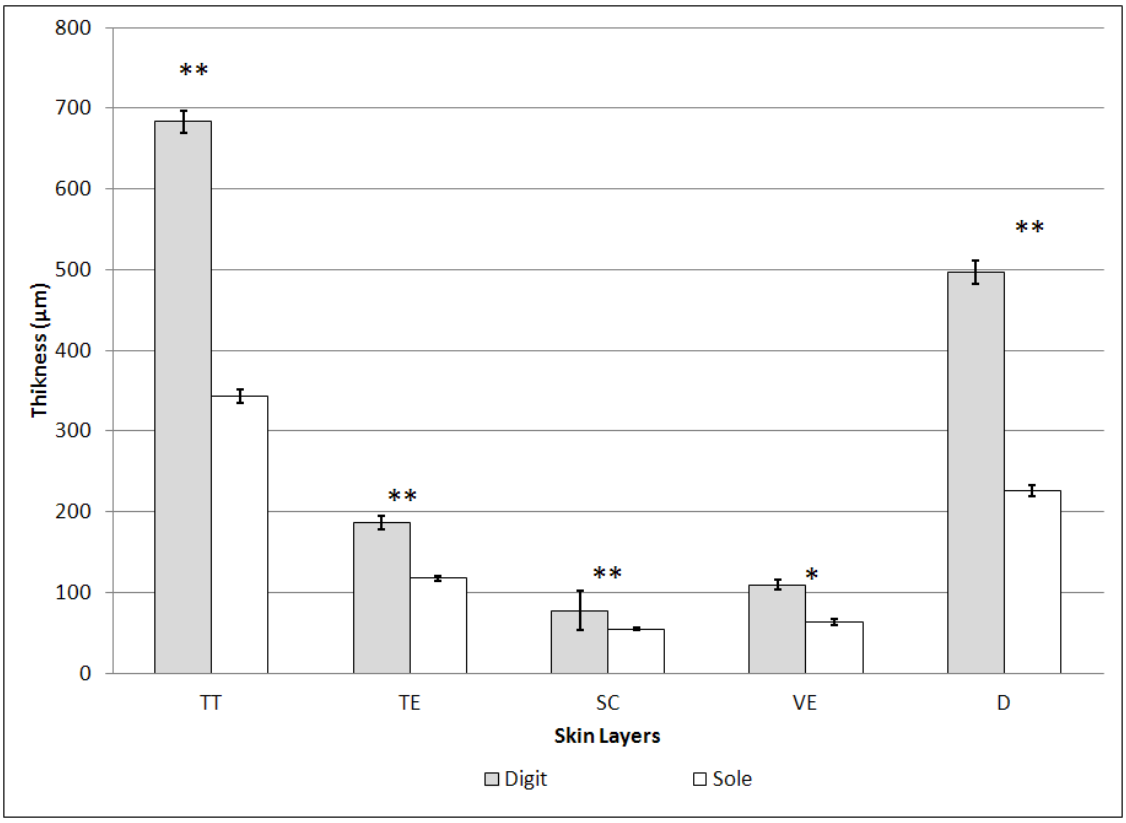

Figure 4.2 Location dependent changes of thickness of the skin layers. TT: Total thickness, TE: Total epidermis, SC: Stratum corneum thickness, VE: Viable epidermis thickness, D: Dermis thickness. (The error bars represent the SEM. **: p<0.0001, *: p<0.001)

After peeling of epidermis after incubation in NaBr, the epidermal cells were almost removed (Figure 4.3 and Figure 4.4). After peeling, the thickness of the total epidermis decreased from 186.41μm to 18.96μm in digit. In the sole, while the thickness of total epidermis was 117.47μm, the thickness of the remaining epidermis after peeling

was 23.80μm. Paired t-test results show that this difference in thickness of epidermis between normal condition and peeled condition was statistically significant ($p<0.0001$ for the digit and $p<0.0001$ for the sole).

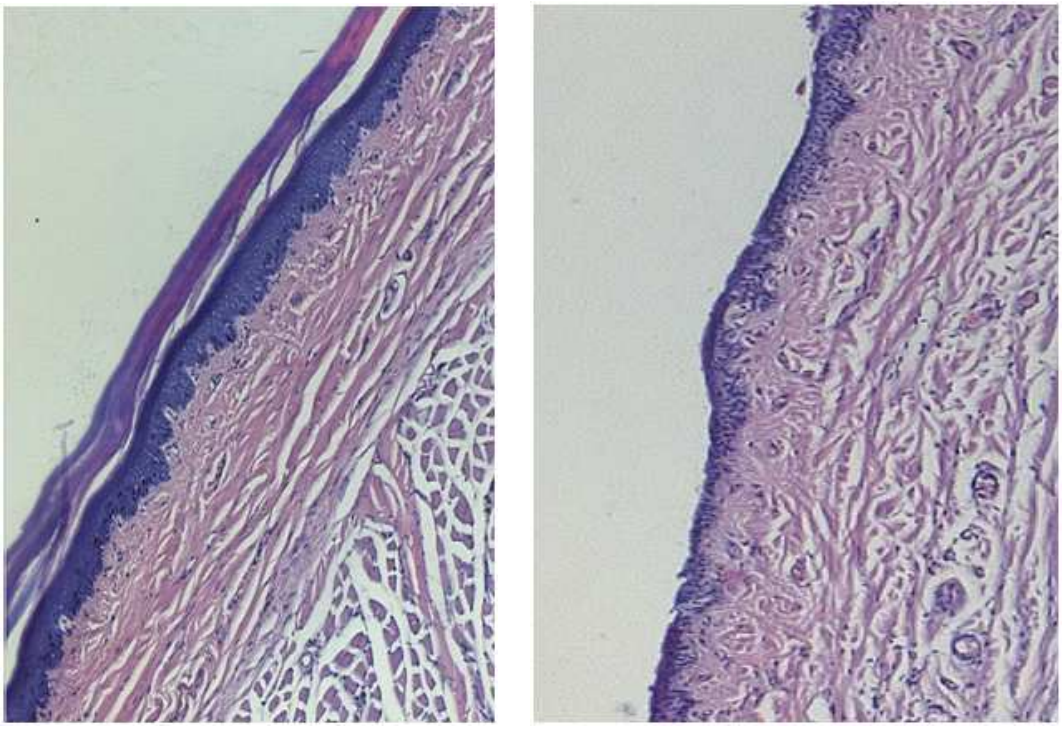

(a) (b)

Figure 4.3 (a) Skin morphology in the normal and (b) the peeled condition.

4.2 Mechanical Impedance

Mechanical Impedance measurements were done at two different frequencies (40 Hz and 250 Hz) and at the same sites studied with histology (digit and sole). All measurements were done in both normal condition and peeled condition.

In the normal condition, the changes in the mechanical impedance components depending on the frequency and the location are shown in Figure 4.5 and Figure 4.6. The resistance in the digit was greater than the sole at both frequencies. For instance, it was about 0.59 Ns/m in the digit at 40 Hz, while it was about 0.48 Ns/m in the sole. Two-way ANOVA results show that difference in the resistance between digit and

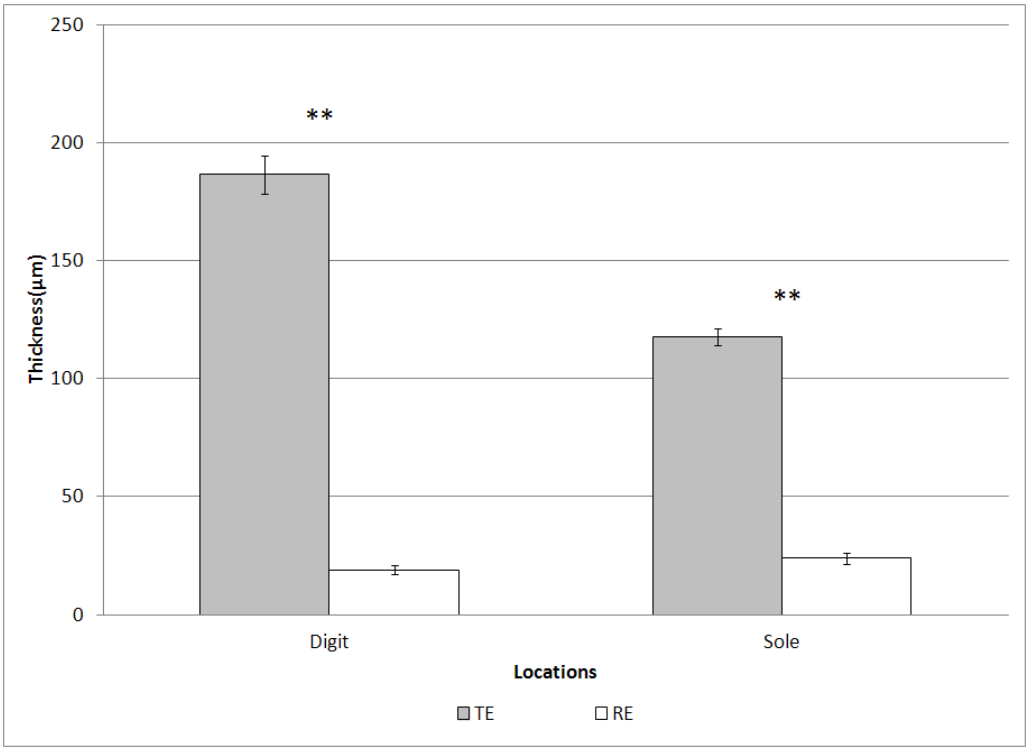

Figure 4.4 Epidermis thickness in normal condition and peeled condition. TE; total epidermis thickness, RE; remaining epidermis thickness after peeling. (The error bars represent the SEM.**: $p<0.0001$)

sole was fairly significant (p=0.056) but the resistance at 40Hz and 250Hz were not significantly different (p=0.376). While the changes in the modulus of the impedance depending on location were not statistically significant (p=0.684), the changes in the modulus of the impedance depending on frequency were found to be statistically significant (p=0.018). At the frequency of 250 Hz, the modulus of the impedance in both digit and sole was about 0.85 Ns/m, while it was about 0.50 Ns/m at the frequency of 40 Hz. Furthermore, both the stimulus frequency and the location had not any significant effect on the reactance(see Table 4.2 for p-values). For all mechanical impedance

Table 4.2
Two-way ANOVA results in the normal condition.

	Resistance	**Reactance**	**Impedance**
Frequency	p=0.376	p=0.484	**p=0.018**
Location	**p=0.056**	p=0.107	p=0.684
Interaction	p=0.870	p=0.321	p=0.639

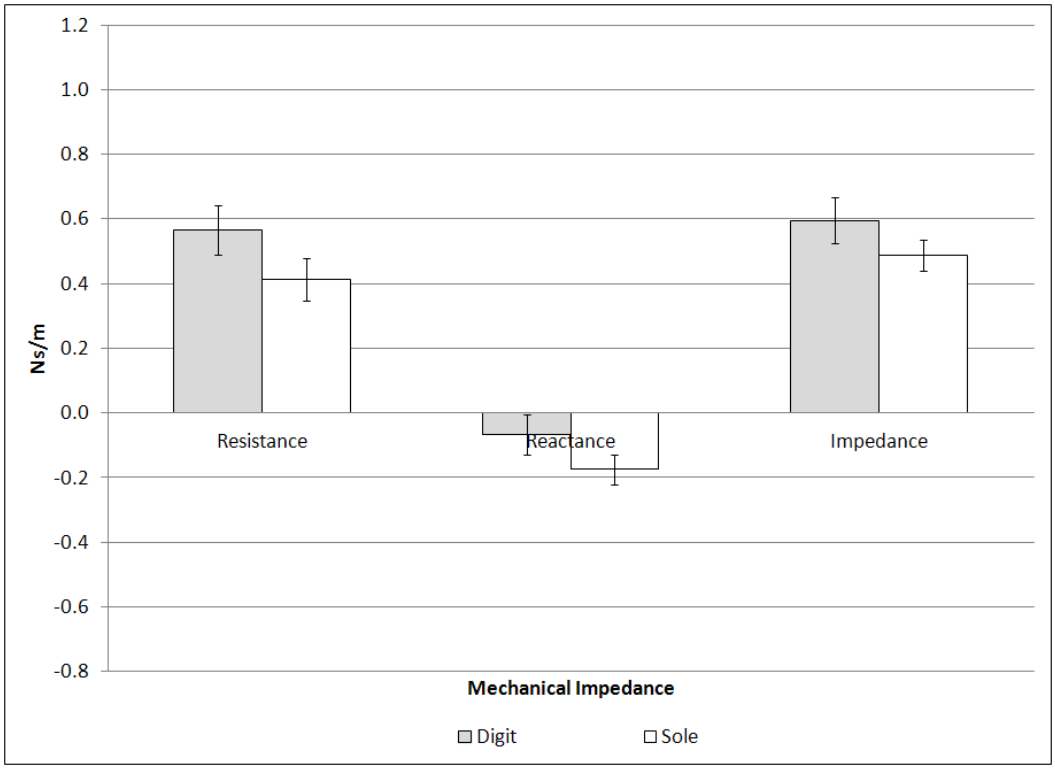

Figure 4.5 Location dependent changes in the mechanical impedance components at 40 Hz in the normal condition. (The error bars represent the SEM.)

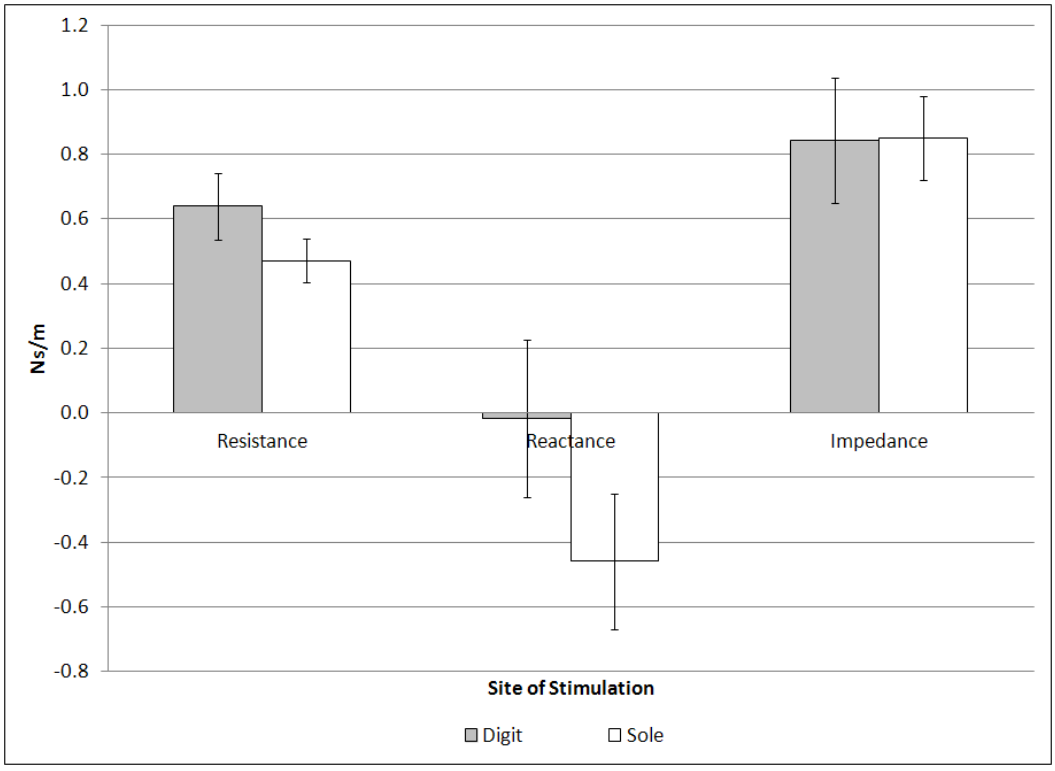

Figure 4.6 Location dependent changes in the mechanical impedance components at 250 Hz in the normal condition. (The error bars represent the SEM.)

Table 4.3
Two-way ANOVA results in peeled condition.

	Resistance	**Reactance**	**Impedance**
Frequency	p=0.197	p=0.613	p=0.658
Location	p=0.892	p=0.218	p=0.354
Interaction	p=0.820	p=0.951	p=0.742

components, there was no interaction effect between location and frequency (see Table 4.2, 2-way ANOVA results).

After peeling of the epidermal layers, the resistance and the modulus of the impedance decreased at the frequency of 40 Hz and 250 Hz. The reactance also became positive at the frequency of 40 Hz and 250 Hz at both locations following the peeling of the epidermal layers (Figure 4.7).

According to paired t-test results, the resistance was significantly different between the normal and the peeled condition at the frequency of 40 Hz in the digit and the sole ($p<0.001$ and $p=0.039$, respectively). In addition, at the frequency of 250 Hz, the resistance in the peeled condition significantly differed from the normal condition in both the digit and the sole ($p<0.001$ and $p=0.005$, respectively).

The reactance in the peeled condition was found to be significantly different from the normal condition at the frequency of 40 Hz in the digit and the sole ($p<0.0001$ and $p<0.001$, respectively). At the frequency of 250 Hz, again the reactance was significantly different between the normal and the peeled condition in the digit and the sole ($p<0.001$ and $p<0.001$, respectively).

Although there was no significantly difference between the moduluses of the impedance in the peeled condition and the normal condition at the frequency of 40 Hz in the digit and the sole ($p=0.434$ and $p=0.411$, respectively), the difference between the moduluses of the impedance between the normal condition and the peeled condition was siginficant at the frequency of 250 Hz in the digit and the sole ($p<0.05$ and $p<0.05$, respectively).

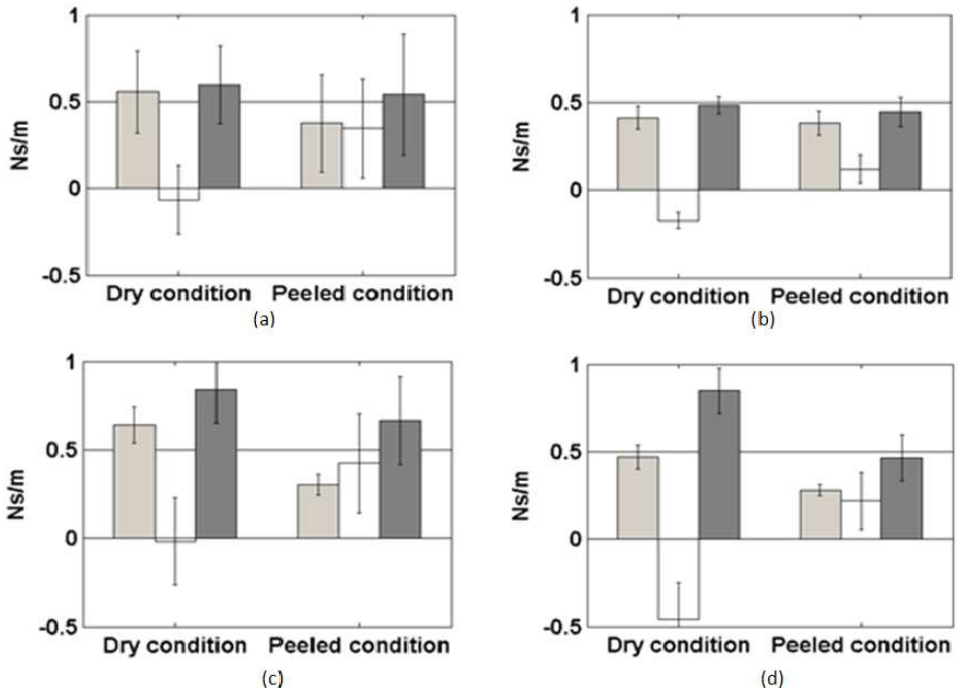

Figure 4.7 Changes in mechanical impedance components in the normal condition and the peeled condition (a) at the frequency of 40 Hz in the digit, (b) at the frequency of 40 Hz in the sole, (c) at the frequency of 250 Hz in the digit, (d) at the frequency of 250 Hz in the sole. (From left to right, bars represents the resistance, reactance and the modulus, respectively. The error bars represent the SEM.)

The changes in the impedance components depending on the frequency and the location are shown in Figure 4.8 and Figure 4.9 for the peeled condition. There were not any significant changes in the resistance, the reactance and the modulus of the impedance at 40 Hz and 250 Hz in the digit and the sole. In the intact skin, the resistance was significantly differed by the location and the modulus of the impedance was changed by the frequency. Two-way ANOVA results in the peeled condition are given in Table 4.3.

4.3 Correlations Between Morphometry and Mechanical Impedance

There were significant correlations between the thickness of the skin layers and the mechanical impedance components at the frequency of 40 Hz as shown in Table 4.4. When all morphometry and mechanical impedance data were considered, there

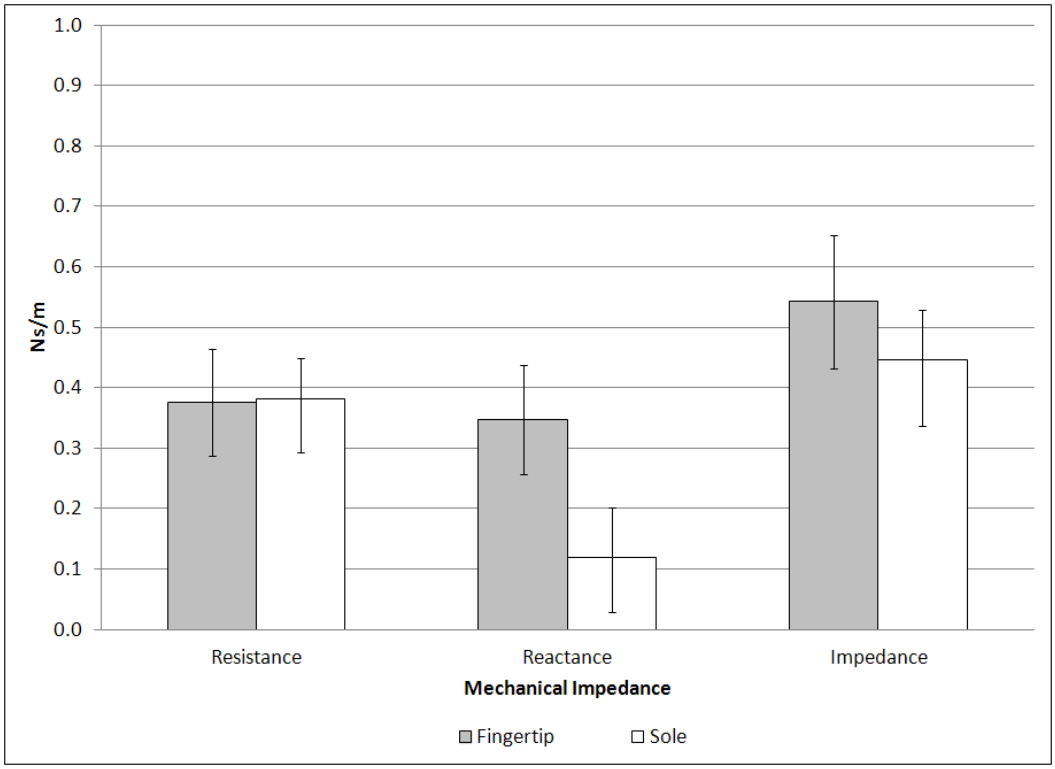

Figure 4.8 Location dependent changes in the mechanical impedance components at 40 Hz in the peeled condition. (The error bars represent the SEM.)

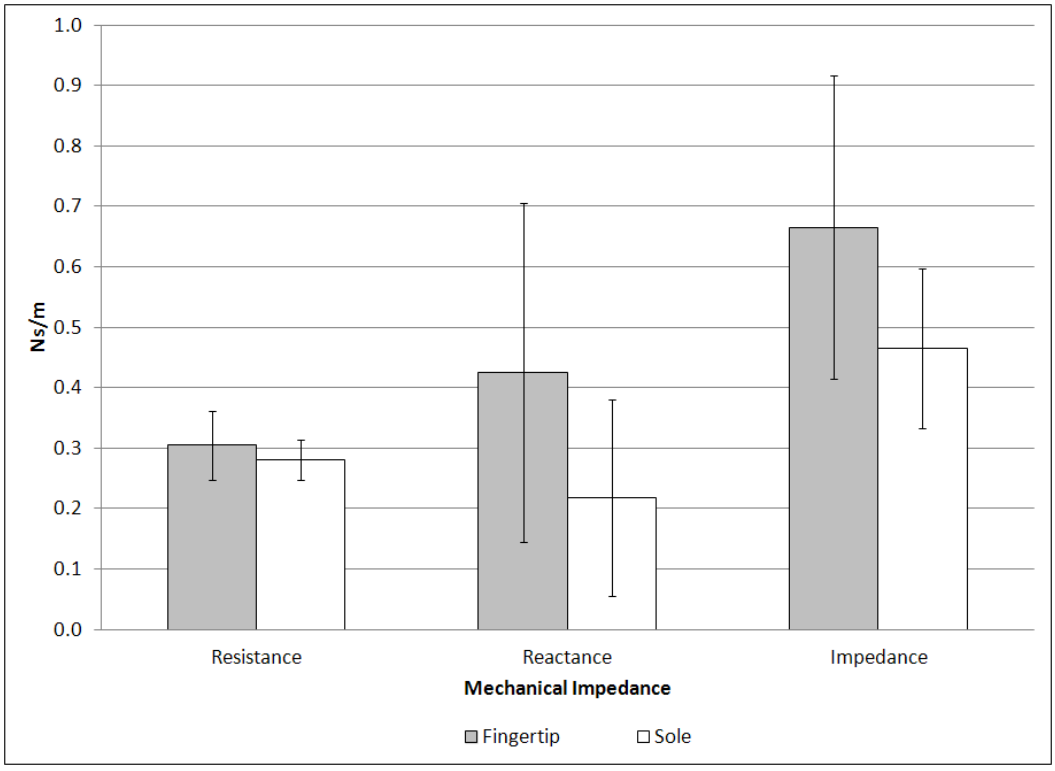

Figure 4.9 Location dependent changes inthe mechanical impedance components at 250 Hz in the peeled condition. (The error bars represent the SEM.)

was a significant correlation between the stratum corneum thickness and the resistance (r=0.61 p=0.06, see Figure 4.10) in the digit. At the maximum value of the stratum corneum thickness which is about 95 μm, the resistance was about 0.4 Ns/m which is the maximum value at 40 Hz in the digit.

Table 4.4
Correlations between the thickness of the skin layers and the mechanical impedance at 40 Hz in the normal condition.

		Resistance	**Reactance**	**Impedance**
Digit	**TT**	r= -0.28	r= -0.35	r= -0.16
		p= 0.43	p= 0.32	p= 0.66
	TE	r= 0.18	r= -0.08	r= 0.17
		p= 0.62	p= 0.83	p= 0.64
	SC	r= 0.61	r= 0.49	r= 0.52
		p= 0.06	p= 0.15	p= 0.12
	VE	r= -0.13	r= -0.40	r= -0.09
		p= 0.72	p= 0.25	p= 0.80
	D	r= -0.36	r= -0.28	r= -0.25
		p= 0.30	p= 0.41	p= 0.49
Sole	**TT**	r= -0.46	r= -0.44	r= -0.37
		p= 0.18	p= 0.19	p= 0.29
	TE	r= 0.28	r= 0.03	r= 0.28
		p= 0.42	p= 0.93	p= 0.43
	SC	**r= 0.94**	**r= 0.92**	**r= 0.86**
		p< 0.0001	**p= 0.0001**	**p= 0.001**
	VE	r= -0.17	r= -0.40	r= -0.12
		p= 0.64	p= 0.25	p= 0.74
	D	**r= -0.68**	r= -0.54	r= -0.58
		p= 0.03	p= 0.10	p= 0.08

Furthermore, in the sole, stratum corneum thickness and all mechanical impedance components were highly correlated and this correlations were statistically significant (r=0.94 p<0.0001 for stratum corneum and resistance, r=0.92 p=0.0001 for stratum corneum and reactance, r=0.86 p=0.001 for stratum corneum and modulus of impedance). The thickness of the dermis was significantly correlated with the resistance at 40 Hz in the sole (r=-0.68 p<0.05)(see Table 4.4).

Table 4.5
Correlations between the thickness of the skin layers and the mechanical impedance measurement at 250 Hz in the normal condition.

		Resistance	Reactance	Impedance
Digit	**TT**	r= -0.08	r= -0.09	r= -0.02
		p= 0.82	p= 0.79	p= 0.95
	TE	r= -0.24	r= -0.43	r= -0.22
		p= 0.50	p= 0.21	p= 0.53
	SC	r= -0.09	r= -0.04	r= -0.03
		p= 0.79	p= 0.90	p= 0.94
	VE	r= -0.27	r= -0.55	r= -0.29
		p= 0.45	p= 0.09	p= 0.42
	D	r= 0.06	r= 0.15	r= 0.10
		p= 0.87	p= 0.671	p= 0.78
Sole	**TT**	r= 0.35	r= 0.15	r= 0.39
		p= 0.32	p= 0.67	p= 0.26
	TE	r= 0.02	r= 0.31	r= 0.13
		p= 0.95	p= 0.37	p= 0.73
	SC	r= -0.11	r= 0.10	r= -0.10
		p= 0.76	p= 0.77	p= 0.78
	VE	r= 0.06	r= 0.21	r= 0.15
		p= 0.88	p= 0.55	p= 0.66
	D	r= 0.40	r= 0.02	r= 0.39
		p= 0.25	p= 0.97	p= 0.26

In the sole, the resistance ranged from 0.1 Ns/m to 0.9 Ns/m. The stratum corneum thickness was between 46 μm and 56 μm in the sole and the sole had thinner dermis which the thickness ranged from 180 μm to 250 μm. The resistance was positively correlated with the stratum corneum thickness (see Figure 4.11), while there was a negative correlation between the dermis thickness and the resistance at 40 Hz in the sole (see Figure 4.12). As given in Figure 4.13 and Figure 4.14, the reactance and the modulus were positively correlated with the stratum corneum thickness at 40 Hz in the sole.

On the other hand, there was no significant correlation between the thickness of the skin layers (total skin, total epidermis, stratum corneum, viable epidermis and dermis th,cknesses) and the resistance, the reactance and the modulus of the impedance at the frequency of 250 Hz as shown in Table 4.5. In other words, at 250Hz the changes in the mechanical impedance components was independent from the thickness of the skin layers.

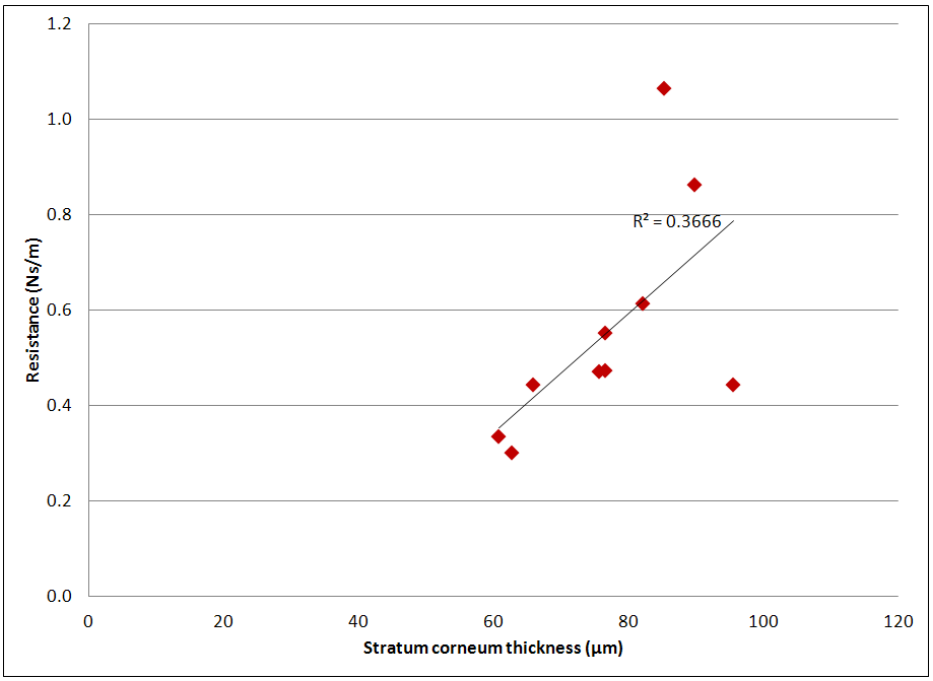

Figure 4.10 Changes in the resistance depending on the thickness of the stratum corneum at 40 Hz in the digit.

After completion of 2M NaBr incubation, epidermis was signficantly removed

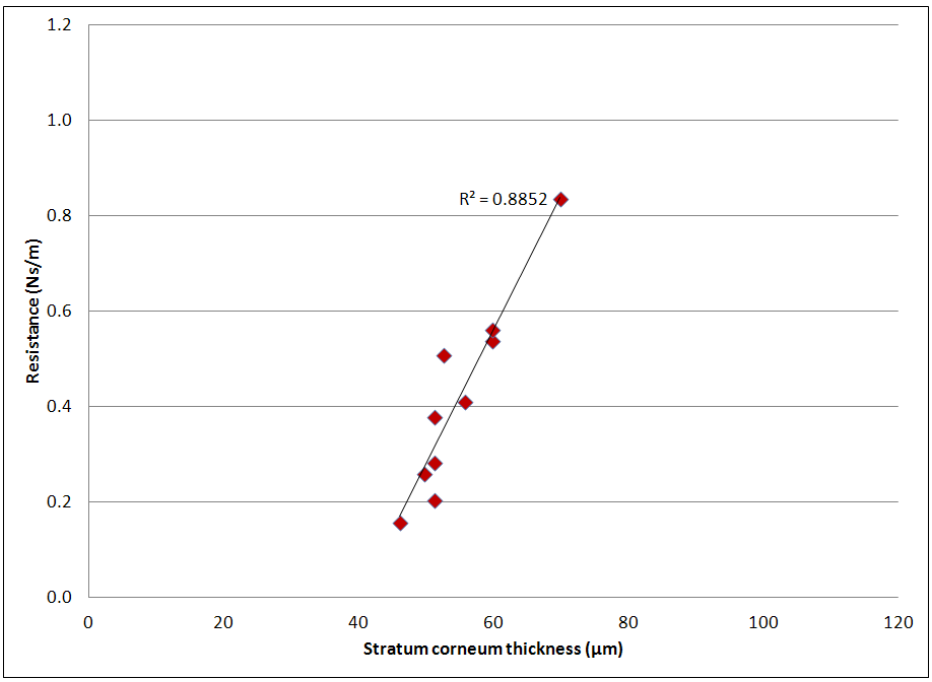

Figure 4.11 Changes in the resistance depending on the thickness of the stratum corneum at 40 Hz in the sole.

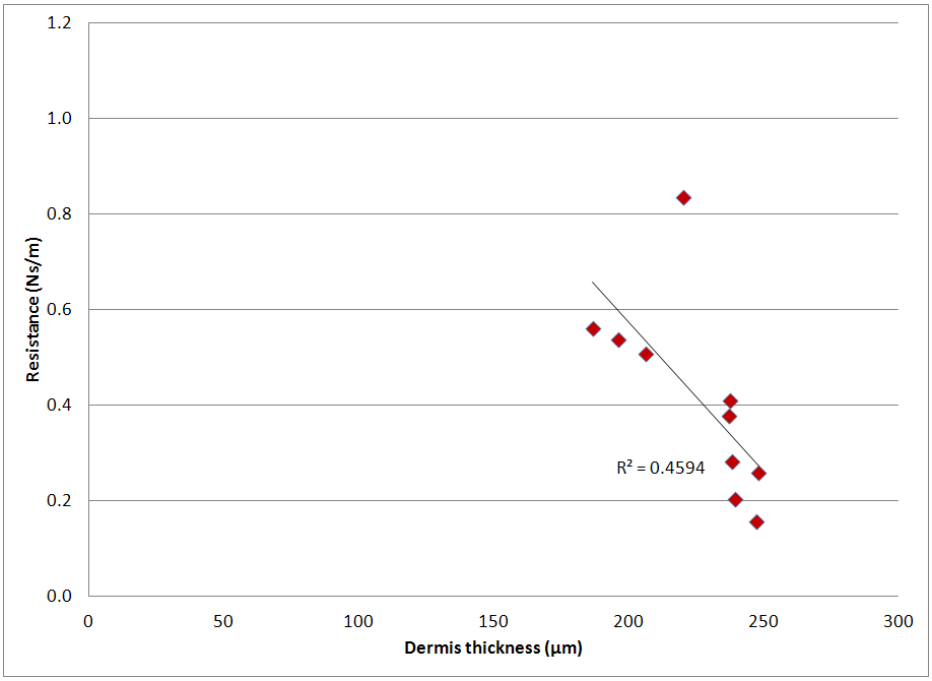

Figure 4.12 Changes in the resistance depending on the thickness of the dermis at 40 Hz in the sole.

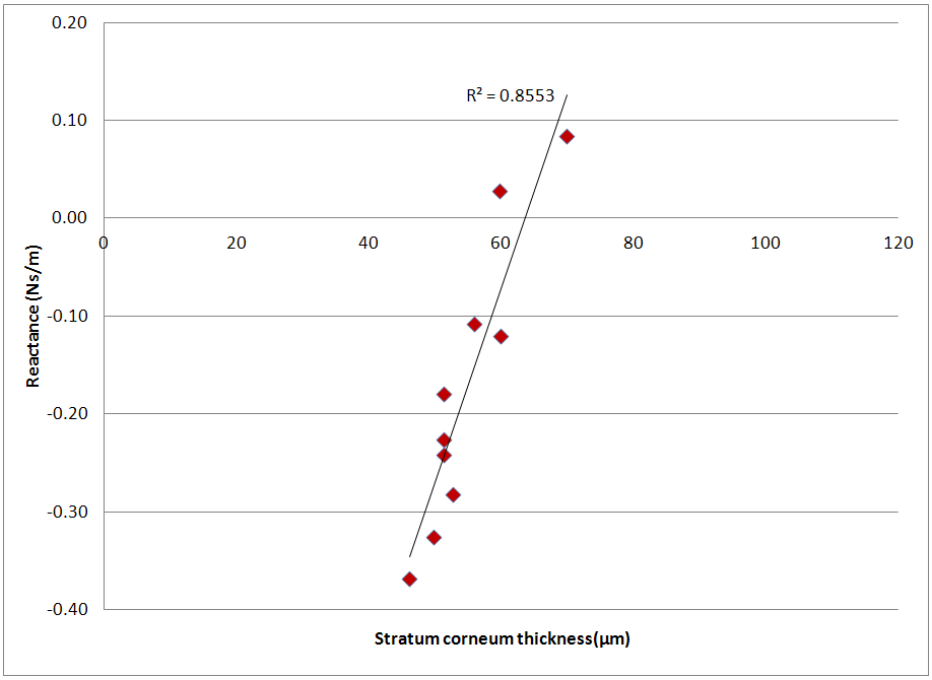

Figure 4.13 Changes in the reactance depending on the thickness of the stratum corneum at 40 Hz in the sole.

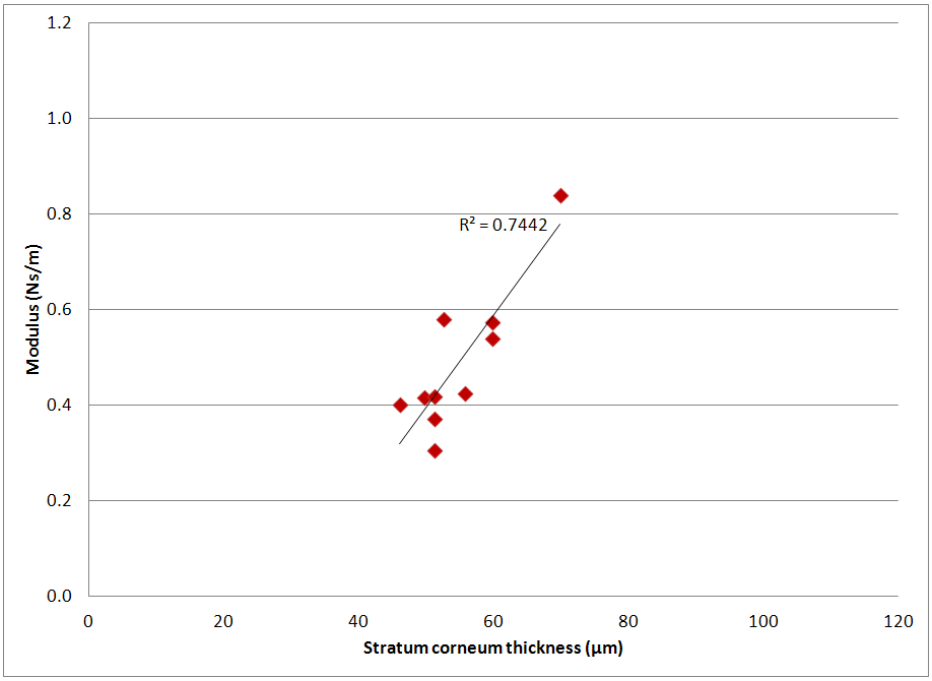

Figure 4.14 Changes in the modulus depending on the thickness of the stratum corneum at 40 Hz in the sole.

in the digit and the sole ($p<0.0001$ for the digit, $p<0.0001$ for the sole). There were significant correlations between the remaining epidermis thickness and the mechanical impedance measurements at the frequency of 40 Hz (see Table 4.6). As given in Figure 4.15(a), the remaining epidermis had positive correlation with the resistance at 40 Hz in the digit. In addition, in the digit, the remaining epidermis thickness was positively correlated with the reactnace and the modulus at 40 Hz (see Figure 4.15(b) and Figure 4.15(c)). Similarly, in the sole, the remaining epidermis thickness had positive correlation with all mechanical impedance components (Figure 4.16).

Table 4.6
Correlation results for thickness of remaining epidermis after peeling and mechanical impedance measurements, RE: remaining epidermis thickness.

			Resistance	**Reactance**	**Impedance**
40 Hz	**Digit**	**RE**	**r= 0.91**	**r= 0.80**	**r= 0.90**
			p<0.001	**p<0.01**	**p<0.001**
	Sole	**RE**	**r= 0.89**	**r= 0.60**	**r= 0.82**
			p<0.001	**p= 0.07**	**p<0.001**
250 Hz	**Digit**	**RE**	r= 0.07	r= 0.18	r= 0.09
			p= 0.85	p= 0.62	p= 0.80
	Sole	**RE**	r= -0.18	r= 0.37	r= 0.28
			p= 0.62	p= 0.30	p= 0.43

The remaining epidermis thickness was not correlated with the mechanical impedance measurements at the frequency of 250 Hz as given in Table 4.6.

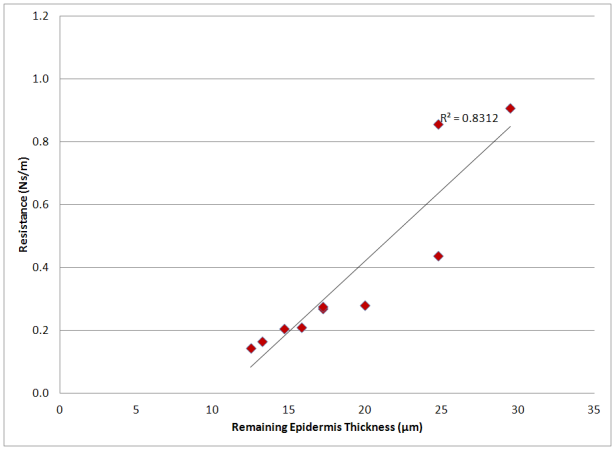

(a)

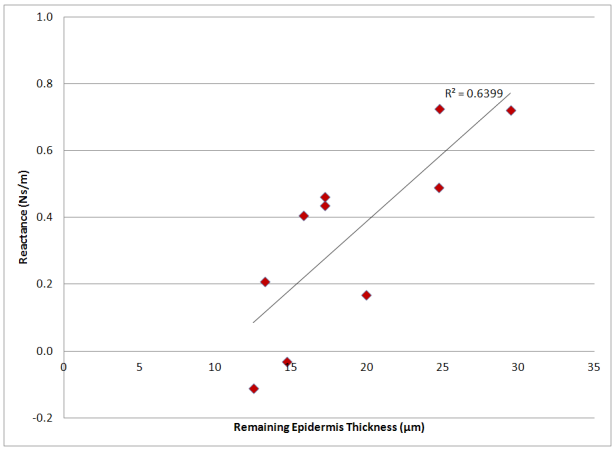

(b)

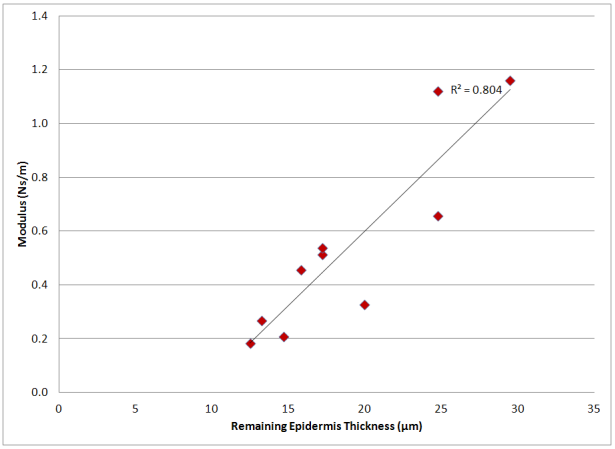

(c)

Figure 4.15 Changes in (a) the resistance (b) the reactance (c) the modulus depending on the remaining epidermis thcikness at 40 Hz in the digit.

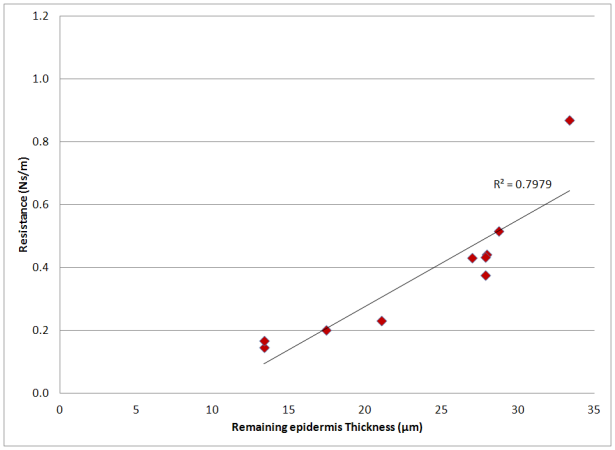

(a)

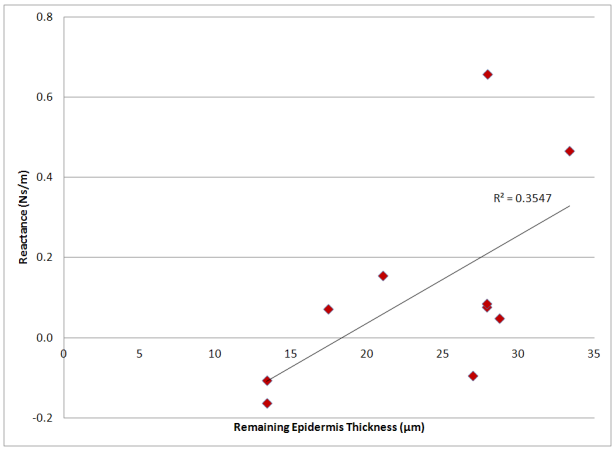

(b)

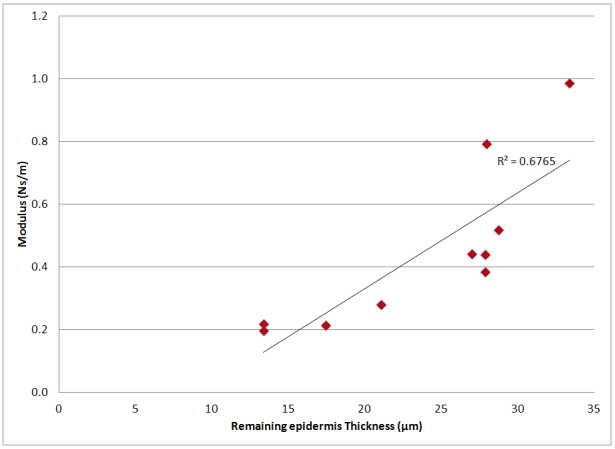

(c)

Figure 4.16 Changes in (a) the resistance (b) the reactance (c) the modulus depending on the remaining epidermis thcikness at 40 Hz in the sole.

5. DISCUSSION

5.1 Skin Mechanics

In thesis presented here, hypothesis that the mechanical impedance components are affected by the frequency of the stimulation and the location stimulated was tested. According to results, the frequency had significant effect on the modulus of the impedance, whereas the resistance and the reactance were not affected by the frequency. The modulus of the impedance at 250 Hz was greater than 40 Hz. Furthermore, while the digit had higher impedance at 40 Hz, the modulus of the impedance was similar in the digit and the sole at 250 Hz. The location stimulated affected just the resistance. The digit had higher resistance than the sole at both 40 Hz and 250 Hz.

The differences attributable to varying site of stimulation and frequency were investigated. In both frequencies, the impedance of skin was found to be governed by the resistance. This finding is in agreement with the findings of Devecioğlu (2011) [17]; however, the impedance measurements of Güçlü and Bolanowski (2005) [16] was governed by the reactance of the skin. The reason for the difference between these two findings may be the size of contactor relative to the digit size and the different subject species.

It is expected that the mechanical impedance components was changed by either the frequency or the location. In the results of Lundström's research in human subjects, ten different points (see Figure 5.1) on the hand were studied. According to his findings, for instance, at 100 Hz, these ten different points had different impedance values. The central part of the palm (point 9) had the lowest impedance which was around 7 Ns/m at 100 Hz; however the two distal points (point 1 and 2) had the highest impedance which was about 22 Ns/m. This difference in the mechanical impedance of the different points at same frequency was attributable to varying location. Additionally, while the fingertip (point 1) had the highest resonance frequency (200Hz), the hypothenar (point 8) and the thenar (point 10) had the lowest resonance frequency (100Hz and 110Hz, respectively) [5]. In the study here, the resonance frequency was

not determined but the modulus of the impedance was also significantly altered by the frequency. The discrepancy between this study and Lundström's study is the range of the data obtained. His data ranged from 25 Ns/m to 30 Ns/m in the distal points of the digit at 40 Hz; however, the mechanical impedance measurement in this thesis was about 0.5 Ns/m. This difference may result from the different subject species and the size of contactor. He worked on human subjects and the size of the contactors used were 0.5 cm^2 and 1 cm^2. The size of the contactor is small relative to the size of the digit in human. The rats were used in this study and the size of the contactor was 0.74 mm in diameter.

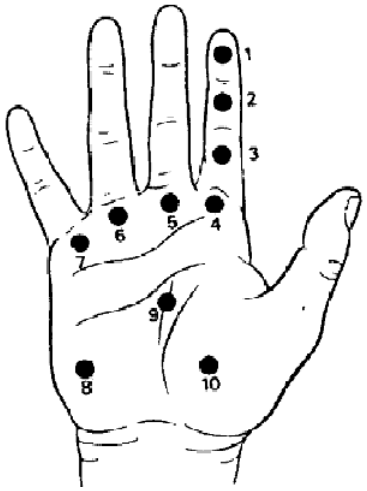

Figure 5.1 Stimulation points in Lundström's study [5].

In the Franke's study, it has shown that the frequency increased, the influence of elasticity decreased and influence of mass increased on the thigh. While the reactance which is the attributable to elasticity was negative at 10 Hz, it became positive at 40 Hz [9]. In this study, at 40 Hz, the reactance was negative in the digit and the sole, and elastic behaviour was dominant. The thigh has stiffer structure than the digit and the sole. Again, the subject species and contactor size were different in these two studies.

In the study presented here, it was that the resistance, the reactance and the modulus of the impedance were varied by the site of stimulation but only the resistance between the digit and the sole was statistically significantly different. In the digit, the skin behaves more resistive. This more resistive behavior of the skin in the digit may

result from the differences in skin-tissue system. The reactance and the modulus of the impedance was similar in the digit and the sole in present study and this result was in agreement with previous study of Moore and Mundie (1972) [8]. According to the findings of Moore and Mundie (1972) , the finger and the thenar eminence were very similar in the reactance and the modulus of impedance.

Mann and Griffin studied the effect of the location of contact with the finger in human subjects. They stimulated 6 different points on the finger: the tip of the finger, the center of the distal phalanx, the distal interphalangeal joint, the center of the middle phalanx, the proximal interphalangeal joint and the center of the proximal phalanx [12]. The behaviour of the skin in the center of the phalanx was similar with the stimulation points in this study. From 40 Hz to 250 Hz, the modulus of the impedance increased in the center of the distal phalanx. In contrast to the behavior of the skin in the digit and the sole at 40 Hz, the modulus is greater at 250 Hz.

5.2 Skin Morphometry

The digit and the sole were chosen as stimulation points because they are also most frequently studied in tactile psychophysics. In the literature, there is not adequate information on the morphometrical properties of rat glabrous skin and the thickness of the layers were not quantified before. On the other hand, by comparison with findings of Ibrahim et al. (2004) [58] and Huang et all. (2008) [59], the thicknesses of the total epidermis, the stratum corneum and the viable epidermis were consistent with the literature.

Other hypothesis tested in here is that the morphometrical parameters (the thickness of the skin layers) are different in the digit and the sole. The structure and the morphometry of glabrous skin and the underlying tissue composition of the digit is different from the sole. The thickness of the epidermal layers and dermis in the digit is greater than the sole thickness. Total thickness of the digit skin is about 683 μm, whereas the sole skin is about 343 μm.

5.3 Relationship between the Mechanical Properties of the Skin and the Morphometrical Measurements

In the presented study here, the association between skin-tissue morphometry and mechanical characteristics of skin were investigated. The mechanical impedance results in the normal condition show that the site of stimulation altered on the resistance of the skin. The digit behaved more resistive. When the digit was compared morphometrically with the sole, the epidermal layers and the dermis in the digit are thicker than those of the sole. This difference in the morphometry may not be enough to gain knowledge about which layer exactly contributes to this resistive behavior; however, the correlation results have shown that stratum corneum thickness was correlated with mechanical impedance measurements at the frequency of 40 Hz.

The second approach in this study was partially or completely peeling the epidermal layers. This provided us with an idea regarding the association between remaining epidermis thickness and mechanical impedance measurements. According to our findings, after peeling the epidermal layers off, the resistance of the skin decreased and there was a positively and statistically significant correlation between the remaining epidermis thickness and the mechanical impedance components at the frequency of 40Hz. These two results suggest that stratum corneum which is the uppermost layer may determine the mechanical properties of skin.

Reactance is the imaginary part of mechanical impedance and it is determined by both the elasticity and the mass of tissue stimulated. When the measured reactance is negative it is dependent primarily upon the elasticity of the tissue stimulated and may be modeled by a spring. Positive reactance is due to the mass of tissue stimulated. In the normal condition, the reactance of tissue was negative and following the peeling of epidermal layers it became positive. A possibility that in the normal condition, the measured mechanical impedance might be mainly due to epidermis, while dermis behaves as a mechanical ground point. Following the peeling, since the dermis is exposed, the measured mechanical impedance may be due to the dermis. Therefore, while dermis behaves like a mass, epidermis may behave like spring.

5.4 Limitations of the Study

Mechanical impedance was measured at two different locations by using same contactor (0.74 mm in diameter). Contactor size covered almost the entire surface the digit skin, hence the measurement was not point contact impedance. In the digit, the mechanical behavior of the entire digit was probably measured. In the sole, working area was much larger than the contactor size and the measurements can be considered completely point contact impedance.

Furthermore, NaBr incubation protocol was used for the peeling of epidermal layers. This method is commonly used in electron microscopy studies for tha qualitative and the quantative analysis of specific cells in epidermis by splitting the epidermal layers. In present study, this method was used for another purpose and it has not been reported in the literature for such purpose. Thus, there is not much information about the side effects of this method on the mechanical behavior of the skin. 2M is highly concentrated salt solution, in particular the concentration of the NaBr used in this research is about twenty times of physiological saline concentration. It may possible that the 2M NaBr solution affected or changed the mechanical properties of the skin.

5.5 Future Work

Basically, the findings of this thesis may be useful for understanding of the mechanical characteristics of glabrous skin and the morphological factors affecting the mechanical behavior of the glabrous skin in its natural condition, developing new mechanical models for the glabrous skin and the haptic devices. Healthy animals were used in the present study, diseased animal models can be used in order to understand the changes in the mechanical characteristics of skin. For instance, the impairment of skin structure and the changes in the mechanical properties of skin may be studied in diabetic animals because diabetes is a progressive metabolic disorder and causes the loss of the sense of touch.

ï»¿

REFERENCES

1. Ray, H., and G. Doetsch, "Coding of stimulus location and intensity in populations of mechanosensitive nerve fibers of the raccoon: I. single fiber response properties.," *Brain Research Bulletin*, Vol. 25, pp. 517–532, 1989.

2. Bischoff, J. E., E. M. Arruda, and K. Grosh, "Tactile sensibility in the human hand: receptive field characteristics of mechanoreceptive units in the glabrous skin area.," *Journal of Physiology*, Vol. 281, pp. 101–125, 1978.

3. Pubols, B., "Effect of mechanical stimulus spread across glabrous skin of raccoon and squirrel monkey hand on tactile primary afferent fiber discharge.," *Somatosensory Research*, Vol. 4, pp. 273–308, 1987.

4. Vega-Bermudez, F., and K. Johansson, "Sa1 and ra receptive fields, response variability, and population responses mapped with a probe array.," *Journal of Neurophysiology*, Vol. 81, pp. 2701–2710, 1999.

5. Lundstrom, R., "Local vibrations-mechanical impedance of the human hand's glabrous skin.," *Journal of Biomechanics*, Vol. 17, pp. 137–144, 1984.

6. Gierke, H. E. V., "Transformation of vibratory energy through human body tissues.," *Proc. First National Biophys. Conf.*, 1959.

7. Gierke, H. E. V., H. L. Oestreicher, E. K. Franke, H. O. Parrack, and V. V. Witterni, "Physics of vibration in living tissues.," *J. Appl. Physiol.*, Vol. 4, pp. 886–900, 1952.

8. Moore, T. J., and J. R. Mundie, "Measurement of specific mechanical impedance of the skin: Effects of force, site of stimulation, area of probe and presence of surround.," *J. of Acoustical Society of America*, Vol. 4, pp. 577–584, 1972.

9. Franke, E. K., "Mechanical impedance measurements of human body surface.," *USAF WADC, Dayton, Ohio, Tech. Rept. 6469*, 1951.

10. Gilmer, B. V., "The measurement of the sensitivity of the skin to mechanical vibration.," *J. Exp. Psychol.*, Vol. 13, pp. 42–61, 1935.

11. Evans, S. L., and C. A. Holt, "Vibratory sensitivity as affected by local anesthesia.," *J. of Exp. Psychol.*, Vol. 25, pp. 429–438, 1939.

12. Mann, N. A., and M. J. Griffin, "Effects of the contact conditions on the mechanical impedance of the finger.," *Centr. Eur. J. Publ. Hlth.*, Vol. 4, no. 1, pp. 46–49, 1996.

13. Wang, Q., and V. Hayward, "In vivo biomechanics of the fingerpad skin under local tangential traction.," *J. of Biomechanics*, Vol. 40, no. 4, pp. 851–860, 2007.

14. Pan, L., L. Zan, and F. S. Foster, "In vivo high frequency ultrasound assessment of skin elasticity.," *,Proceedings of the IEEE Ultrasonics Symposium*, no. , PAGES =, 1997.

15. Cauna, N., "Nature and functions of the papillary ridges of the digital skin.," *The Anatomical Record*, Vol. 119, pp. 449–468, 1954.

16. Güçlü, B., and S. J. Bolanowski, "Vibrotactile thresholds of non-pacinian i channel: predicting the effects of contactor location on the phalanx.," *Somatosensory Research*, Vol. 22, pp. 57–68, June 2005.

17. Devecioğlu, İ., "Effects of contactor size and stimulation distance the response properties of ra tactile fibers innervating the rat glabrous skin.," *Master's Thesis, Institute of Biomedical Engineering, BogaziÃ§i University*, 2011.

18. Proksch, E., "The skin: An indispensable barrier.," *Exp. Dermatol.*, Vol. 17, no. 12, 2008.

19. Gardner, E. P., J. H. Martin, and T. M. Jessell, *in Principle of Neural Science 4th ed.*, New York, USA: McGraw-Hill, 2000.

20. Gwakrodger, D. J., *Dermatology; An illustrated colour text 3rd Edition*, 2002.

21. Tortora, G., and B. Derrickson, *Principles of Anatomy and Physiology*, Hoboken: John Wiley, 2009.

22. Plewig, G., and R. R. Marples, "Regional differences of cell sizes in the human stratum corneum.," *British Journal of Dermatology*, Vol. 54, no. 1, pp. 13–18, 1970.

23. Holbrook, K. A., and G. F. Odland, "Regional differences in the thickness (cell layers) of the human stratum corneum: an ultrastructural analysis.," *Journal of Investigative Dermatology*, Vol. 62, no. 4, pp. 415–422, 1974.

24. Holbrook, K. A., and G. F. Odland, "Ultrastructure of the stratum corneum.," *International Journal of Dermatology*, Vol. 16, no. 4, pp. 245–256, 1977.

25. Agache, P., and P. Humbert, "Cutaneous receptors," in *Measuring the skin*, Berlin: Springer Verlag, 2004.

26. Plewig, G., and R. R. Marples, "Regional differences of cell sizes in the human stratum corneum. ii. effects of sex and age.," *British Journal of Dermatology*, Vol. 54, no. 1, pp. 19–23, 1970.

27. Rawlings, A. V., L. R. Scott, C. R. Harding, and P. A. Bowser, "Stratum corneum moisturization at the molecular level.," *Journal of Investigative Dermatology*, Vol. 103, no. 5, pp. 731–740, 1994.

28. Agache, P., J. P. Boyer, and R. Laurent, "Stratum corneum moisturization at the molecular level.," *Archives of Dermatological Research*, Vol. 246, no. 3, pp. 271–283, 1973.

29. Elias, P. M., "Stratum corneum defensive functions: an integrated view.," *British Journal of Dermatology*, Vol. 125, no. 2, pp. 183–200, 2005.

30. Sandby-Moller, J., H. C. Wulf, and T. Poulsen, "Epidermal thickness at different body sites: Relationship to age, gender, pigmentation, blood content, skin type and smoking habits.," *Acta Dermato-Venereologica*, Vol. 83, no. 6, pp. 410–413, 2003.

31. Silver, F. H., L. M. Siperko, and G. P. Seehra, "Mechanobiology of force transduction in dermal tissue.," *Skin Research and Technology*, Vol. 9, no. 1, pp. 3–23, 2003.

32. Ebling, F., R. Eady, I. Leigh, R. H. Champion, J. L. Burrington, and F. J. Ebling, *Anatomy and organization of human skin.*, New York: Blackwell Scientific Publications, 1992.

33. Finlay, B., "Scanning electron microscopy of the human dermis under uni-axial strain.," *Bio-medical Engineering*, Vol. 4, pp. 322–327, 1969.

34. Oxlund, H., J. Manschot, and A. Viidik, "The role of elastin in the mechanical properties of skin.," *Journal of Biomechanics*, Vol. 21, no. 3, pp. 213–218, 1988.

35. Avram, A. S., M. M. Avram, and W. D. James, "Subcutaneous fat in normal and diseased states: 2. anatomy and physiology of white and brown adipose tissue.," *Journal of the American Academy of Dermatology*, Vol. 53, no. 4, pp. 671–683, 2005.

36. Birznieks, I., P. Jenmalm, A. W. Goodwin, and R. S. Johansson, "Encoding of direction of fingertip forces by human tactile afferents.," *Journal of Neuroscience*, Vol. 21, pp. 8222–8237, 2001.

37. Moy, G., U. Singh, E. Tan, and R. Fearing, "Human psychophysics for teletaction system design.," . *Haptics-e*, Vol. 1, no. 3, 2000a.

38. Park, A. C., and C. B. Baddiel, "Rheology of stratum corneum-i: A molecular interpretation of the stress-strain curve.," *Journal of Society Cosmetical Chemistry*, pp. 233–245, 1972.

39. Papir, Y. S., K. H. Hsu, and R. H. Wildnauer, "The mechanical properties of stratum corneum. i. the effect of water and ambient temperature on the tensile properties of newborn rat stratum corneum.," *Biochimica et Biophysica Acta*, Vol. 399, no. 1, pp. 170–180, 1975.

40. Wolfram, M. A., N. F. Wolejsza, and K. Laden, "Biomechanical properties of delipidized stratum corneum.," *British Journal of Dermatology*, Vol. 59, no. 6, pp. 421–426, 1972.

41. Duzee, B. F. V., "The influence of water content, chemical treatment and temperature on the rheological properties of stratum corneum.," *Journal of Investigative Dermatology*, Vol. 71, no. 2, pp. 140–144, 1978.

42. DeRigal, J., and J. L. Leveque, "In vivo measurement of the stratum corneum elasticity.," *Bioengineering and the Skin*, Vol. 1, no. 1, pp. 13–23, 1985.

43. Agache, P. G., C. Monneur, J. L. Leveque, and J. DeRigal, "chanical properties and young's modulus of human skin in vivo.," *Archives of Dermatological Research*, Vol. 269, no. 3, pp. 221–232, 1980.

44. Leveque, J. L., J. DeRigal, P. G. Agache, and C. Monneur, "Influence of ageing on the in vivo extensibility of human skin at a low stress," *Archives of Dermatological Research*, Vol. 269, no. 2, pp. 127–135, 1980.

45. Pierard, G. E., N. N. Tassoudji, and C. P. Franchimont, "Influence of the test area on the mechanical properties of skin.," *Dermatology*, Vol. 19, no. 1, pp. 9–15, 1995.

46. Gardner, T. N., and G. A. Briggs, "Biomechanical measurements in microscopically thin stratum corneum using acoustics.," *Skin Research and Technology*, Vol. 7, no. 4, pp. 254–261, 2001.

47. Kendall, M. A., Y. F. Chong, and A. Cock, "The mechanical properties of the skin epidermis in relation to targeted gene and drug delivery.," *Biomaterials*, Vol. 28, no. 33, pp. 4968–4977, 2007.

48. Hendriks, F. M., C. W. Oomens, D. L. Bader, F. P. Baaijens, and D. Brokken, "The relative contributions of different skin layers to the mechanical behavior of human skin in vivo using suction experiments.," *Medical Engineering and Physics*, Vol. 28, no. 3, pp. 259–266, 2006.

49. Patel, P. N., C. K. Smith, and C. W. Patrick, "Rheological and recovery properties of poly(ethylene glycol) diacrylate hydrogels and human adipose tissue.," *Journal of Biomedical Materials Research Part A*, Vol. 73A, no. 3, pp. 313–319, 2005.

50. Manschot, J., "The mechanical properties of human skin in vivo.," *Ph.D. thesis, Catholic University of Nijmegen*, 1985.

51. Maurel, W., Y. Wu, N. M. Thalmann, and F. Thalmann, "Biomechanical models for soft tissue simulation.," in *Esprit Basic Research Series*, pp. 5–22, Berlin: Springer-Verlag, 1998.

52. Lokshin, O., and Y. Lanir, "Viscoelasticity and preconditioning of rat skin under uniaxial stretch: Microstructural constitutive characterization.," *Journal of Biomechanical Engineering*, Vol. 131, no. 3, 2009.

53. Delalleau, A., G. Josse, J. M. Lagarde, H. Zahouani, and J. M. Bergheau, "A nonlinearelastic behavior to identify the mechanical parameters of human skin in vivo.," *Skin Research and Technology*, Vol. 14, pp. 152–164, 2008.

54. Yun, J. S., and W. Montana, "The skin of primates xxv. melanogenesis in the skin of the bushbabies.," *Am. J. Anthropy*, Vol. 23, pp. 143–148, 1951.

55. Starrico, R. J., and H. Pinkus, "Quantative and qualitative data on the pigment cells of adult human epidermis.," *J. of Inv.Derm*, Vol. 28, pp. 33–45, 1957.

56. Avwioro, G., "Histochemical uses of hematoxylin.," *JPCS*, pp. 24–34, 2011.

57. Kiernan, J. A., *Histological and Histochemical Methods: Theory and Practice. 4th ed.*, UK: Scion: Bloxham, 2008.

58. Ibrahim, M. M., F. Porreca, J. Lai, F. L. R. P J. Albreicht, A. Khodorova, G. Davar, A. Makriyannis, T. W. Vanderah, H. P. Mata, and P. JrMalan, "Cb2 cannabinoid receptor activation produces antinociception by stimulating peripheral release of endogenous opoids.," *PNAS*, Vol. 102, no. 8, pp. 3093–3098, 2004.

59. Huang, S. M., H. Lee, M. K. Chung, U. Park, Y. Y. Yu, H. B. Bradshaw, P. A. Coulombe, and J. M. Walker, "Overexpressed transient receptor potential vanilloid-3 ion channels in skin keratinocytes modulate pain sensitivity via prostoglandin e2.," *The Journal Of Neuroscience*, Vol. 28, no. 51, pp. 13727–13737, 2008.